

Type-I Seesaw with eV-Scale Neutrinos

G. C. Branco ^{a,b 1}, J. T. Penedo ^{a 2}, Pedro M. F. Pereira ^{a 3},
M. N. Rebelo ^{a,b 4}, and J. I. Silva-Marcos ^{a 5}

^a Centro de Física Teórica de Partículas, CFTP, Departamento de Física,
Instituto Superior Técnico, Universidade de Lisboa,
Avenida Rovisco Pais nr. 1, 1049-001 Lisboa, Portugal;

^b CERN, Theoretical Physics Department, *CH-1211 Geneva 23, Switzerland.*

Abstract

We consider seesaw type-I models including at least one (mostly-)sterile neutrino with mass at the eV scale. Three distinct situations are found, where the presence of light extra neutrinos is naturally justified by an approximately conserved lepton number symmetry. To analyse these scenarios consistently, it is crucial to employ an exact parametrisation of the full mixing matrix. We provide additional exact results, including generalised versions of the seesaw relation and of the Casas-Ibarra parametrisation, valid for every scale of seesaw. We find that the existence of a light sterile neutrino imposes an upper bound on the lightest neutrino mass. We further assess the impact of light sterile states on short- and long-baseline neutrino oscillation experiments, emphasise future detection prospects, and address CP Violation in this framework via the analysis of CP asymmetries and construction of weak basis invariants. The proposed models can accommodate enough active-sterile mixing to play a role in the explanation of short-baseline anomalies.

PACS numbers : 12.15.Ff, 14.60.Pq, 14.60.St

¹E-mail: gbranco@tecnico.ulisboa.pt

²E-mail: joao.t.n.penedo@tecnico.ulisboa.pt

³E-mail: pedromanuelpereira@tecnico.ulisboa.pt

⁴E-mail: rebelo@tecnico.ulisboa.pt. On leave of absence from ^a CFTP/IST, U. Lisboa

⁵E-mail: juca@cftp.tecnico.ulisboa.pt

1 Introduction

Most of the present data on Neutrino Physics are consistent with the hypothesis of having only three active neutrinos. Nevertheless, there is a small subset of experiments which seem to require the presence of New Physics (NP). The first indication hinting at the presence of NP was provided by an excess in the results of the LSND experiment, where electron anti-neutrinos were observed in a pure muon anti-neutrino beam [1,2]. One of the simplest explanations of the LSND result involves the existence of an anti-neutrino with a mass-squared difference Δm^2 of about 1 eV^2 . Taking into account that Δm_{atm}^2 is of order 10^{-3} eV^2 and $\Delta m_{\text{solar}}^2$ of order 10^{-4} eV^2 one concludes that the LSND result would require a fourth neutrino. On the other hand, the invisible decay of the Z gauge boson shows that there are only three active neutrinos with a mass less than a half of the Z mass [3], implying that if a fourth light neutrino exists it must be sterile, i.e., a singlet under the gauge symmetry of the Standard Model (SM). The existence of extra (sterile) neutrinos should then be reconciled with cosmological constraints, which call for a suppressed thermalisation of these massive neutrinos in the early Universe, given the effective neutrino number $N_{\text{eff}} = 2.99^{+0.34}_{-0.33}$ (95% CL, from TT,TE,EE+lowE+lensing+BAO) measured by Planck [4]¹.

Meanwhile, new anomalies have appeared in Neutrino Physics supporting the hypothesis of the existence of light sterile neutrinos. The indications for the existence of a sterile neutrino of mass of order 1 eV come from short-baseline (SBL) neutrino oscillation experiments. They started with the LSND result in the nineties. At that time, this result was not confirmed by KARMEN [7]. However, KARMEN had a shorter baseline than LSND and therefore could not exclude the whole parameter space available to LSND. This was followed by the MiniBooNE experiment [8] with inconclusive results². Recently, new interest in the LSND result was sparked by the “reactor anti-neutrino anomaly” due to a deficit of the number of anti-neutrinos observed in several different reactor neutrino experiments, when compared with the theoretical flux calculations [12–14]. A crucial and independent development has been provided by the DANSS [15] and NEOS [16] collaborations, whose programmes include comparing spectra at different distances from the anti-neutrino source. The preferred fit regions of these independent experiments interestingly overlap near $\Delta m^2 \sim 1.4 \text{ eV}^2$ and $\sin^2 2\vartheta_{14} \sim 0.05$, with ϑ_{14} being an effective mixing angle as interpreted in a 3+1 scheme. Also of relevance is the so-called “Gallium neutrino anomaly”, discovered in 2005-2006 [17–19], albeit of less significance. For recent reviews on eV-scale sterile neutrinos and additional references, see [20, 21].

The purpose of this paper is to investigate the possibility of obtaining in a natural way at least one sterile neutrino with a mass of order eV in the framework of the general type-I seesaw mechanism [22–26]. The crucial point is that we shall consider a special case of the seesaw framework. Instead of having three heavy sterile neutrinos, as in the usual setup, at least one of the sterile neutrinos should be light while, at the same time, its mixing with the light active neutrinos should be small enough to comply with existing experimental bounds, but large enough to be relevant to low energy phenomenology. Two important challenges are to

¹ Although addressing this suppression falls beyond our scope, it has been shown that it can be achieved via “secret” sterile neutrino self-interactions [5,6]. Here, TT,TE and EE+lowE+lensing refer to particular likelihood combinations and BAO stands for baryon acoustic oscillation measurements.

² The need to reconcile MiniBooNE and LSND data has currently revived interest [9,10] in models attempting to explain anomalies via sterile neutrino decay [11].

find solutions that are stable under renormalisation, and to inquire if these spectra, with at least one neutrino with a mass of order eV, might indeed explain the SBL anomalies.

For definiteness, let us recall how the conventional seesaw mechanism works. It consists of an extension of the SM where three right-handed neutrinos are added to the standard spectrum. As a result, the neutrino mass terms include a Dirac mass matrix, denoted m , generated by the breakdown of the electroweak (EW) symmetry, and a Majorana mass term, denoted M , with the scale of M much larger than the scale of m . In general this leads to three light neutrinos with masses of order m^2/M and three heavy neutrinos with masses of order M . The generic seesaw framework leads to an active-sterile mixing of order m/M , too small to be of relevance to low energy physics, while providing a framework for leptogenesis [27]. In the derivation of the standard seesaw formulae, one performs a block diagonalisation of the 6×6 complex neutrino mass matrix, obtaining approximate relations that are valid to an excellent approximation. Some of the approximate formulae no longer hold in the special cases which we are considering. However, there are important exact relations which continue to be valid in our case. We find viable models with at least one sterile neutrino with a mass of order eV by imposing a $U(1)$ symmetry (see e.g. [28]) allowing for small breaking terms. Before the breaking, for special assignments of leptonic charges, the lightest neutrinos are naturally massless at tree level, acquiring calculable small masses after the breaking and complying with the experimental Δm^2 values after radiative corrections.

The paper is organised as follows. In the next section, we describe our setup, settle the notation and present a useful parametrisation of the mixing matrix as well as some exact results concerning the Dirac mass matrix, neutrino masses and deviations from unitarity. In section 3 we discuss the size of such deviations from unitarity in the 3×3 leptonic mixing matrix. In section 4 we describe how one-loop mass corrections can be controlled within the considered framework. In section 5 we present explicit numeric examples and go through their phenomenology, while section 6 is dedicated to the study of CP Violation within the type-I seesaw, with emphasis on CP Violation measurements and CP-odd weak basis invariants. Finally our conclusions are presented in section 7.

2 Framework

We work under the type-I seesaw framework, in a model with three right-handed neutrinos added to the SM. The leptonic mass terms are given by:

$$\begin{aligned}\mathcal{L}_m &= - \left[\overline{\mathbf{v}}_L^0 m \mathbf{v}_R^0 + \frac{1}{2} \mathbf{v}_R^{0T} C^* M \mathbf{v}_R^0 + \overline{l}_L^0 m_l l_R^0 \right] + \text{h.c.} \\ &= - \left[\frac{1}{2} n_L^{0T} C^* \mathcal{M}^* n_L^0 + \overline{l}_L^0 m_l l_R^0 \right] + \text{h.c.},\end{aligned}\tag{2.1}$$

where $n_L^0 = (\mathbf{v}_L^0, C \overline{\mathbf{v}}_R^{0T})^T$ and the zero superscript denotes a general flavour basis. Without loss of generality, one may choose a weak basis where m_l is real and diagonal. The analysis that follows is performed in this basis, meaning $\mathbf{v}_L^0 = (\mathbf{v}_{eL}, \mathbf{v}_{\mu L}, \mathbf{v}_{\tau L})$. The neutrino mass matrix \mathcal{M}

is a 6×6 complex symmetric matrix and has the form:

$$\mathcal{M} = \begin{pmatrix} 0 & m \\ m^T & M \end{pmatrix}. \quad (2.2)$$

This matrix is diagonalised by the unitary transformation

$$\mathcal{V}^T \mathcal{M}^* \mathcal{V} = \mathcal{D} \quad \Longleftrightarrow \quad \mathcal{M} = \mathcal{V} \mathcal{D} \mathcal{V}^T, \quad (2.3)$$

where \mathcal{D} is diagonal real non-negative and contains all neutrino masses,

$$\mathcal{D} = \begin{pmatrix} d & 0 \\ 0 & D \end{pmatrix}. \quad (2.4)$$

Here, d contains the masses of the three known light neutrinos, $d = \text{diag}(m_1, m_2, m_3)$, and D the masses of other neutrinos, $D = \text{diag}(M_1, M_2, M_3)$. The 6×6 unitary matrix \mathcal{V} can be written as

$$\mathcal{V} = \begin{pmatrix} K & R \\ S & Z \end{pmatrix}, \quad (2.5)$$

where K , R , S and Z are 3×3 matrices. Using the unitarity of \mathcal{V} , namely $\mathcal{V} \mathcal{V}^\dagger = \mathcal{V}^\dagger \mathcal{V} = \mathbb{1}_{(6 \times 6)}$, one can obtain [29] a series of exact relations relating the matrices K , R , S , and Z , examples of which are $KK^\dagger + RR^\dagger = \mathbb{1}$ and $KS^\dagger + RZ^\dagger = 0$. We shall show that in order to study deviations of unitarity, it is useful to parametrise \mathcal{V} in a different way.

2.1 A Novel Parametrisation for the Leptonic Mixing Matrix

In Ref. [29] we introduced an especially useful parametrisation of the 6×6 leptonic mixing matrix that enables to control all deviations from unitarity through a single 3×3 matrix which connects the mixing of the active and sterile neutrinos in the context of type I seesaw. It was written:

$$\mathcal{V} = \begin{pmatrix} K & 0 \\ 0 & Z \end{pmatrix} \begin{pmatrix} \mathbb{1} & Y \\ -X & \mathbb{1} \end{pmatrix}, \quad X = -Z^{-1}S, \quad Y = K^{-1}R, \quad (2.6)$$

where it is assumed that K and Z are non-singular. From the aforementioned unitarity relation $KS^\dagger + RZ^\dagger = 0$ one promptly concludes that

$$Y = X^\dagger \quad \Longrightarrow \quad \mathcal{V} = \begin{pmatrix} K & KX^\dagger \\ -ZX & Z \end{pmatrix}. \quad (2.7)$$

Thus, a generic 6×6 unitary matrix \mathcal{V} , in fact, only contains three effective 3×3 matrices K , Z and X . Furthermore, from the same unitarity of \mathcal{V} and from the singular value decomposition $X = W d_X U^\dagger$, one finds that K and Z can be written as:

$$\begin{aligned} K &= U_K \sqrt{(\mathbb{1} + d_X^2)^{-1}} U^\dagger = U_K U^\dagger \sqrt{(\mathbb{1} + X^\dagger X)^{-1}} = V \sqrt{(\mathbb{1} + X^\dagger X)^{-1}}, \\ Z &= W_Z \sqrt{(\mathbb{1} + d_X^2)^{-1}} W^\dagger = W_Z W^\dagger \sqrt{(\mathbb{1} + X X^\dagger)^{-1}}, \end{aligned} \quad (2.8)$$

where³ U_K, W_Z, U and W are all 3×3 unitary matrices, d_X is a diagonal matrix with real non-negative entries, and we have defined an additional unitary matrix $V \equiv U_K U^\dagger$. The matrices U and W diagonalise the Hermitian products $X^\dagger X$ and XX^\dagger , respectively:

$$U^\dagger X^\dagger X U = d_X^2, \quad W^\dagger X X^\dagger W = d_X^2. \quad (2.9)$$

Any unitary matrix to the left of Z – like the product $W_Z W^\dagger$ in Eq. (2.8) – is unphysical as it can be rotated away via a weak basis transformation which does not affect the form of m_l . Accordingly, one can choose to work in a weak basis for which $\Sigma = \mathbb{1}$ in the general expression

$$Z = \Sigma (\mathbb{1} + X X^\dagger)^{-1/2}, \quad (2.10)$$

with Σ unitary. Note, however, that $\Sigma \neq \mathbb{1}$ in the numerical ‘symmetry’ bases considered later on in sections 4 and 5.

The matrix K plays the role of the PMNS mixing matrix, as it connects the flavour eigenstates $\nu_{\alpha L}$ ($\alpha = e, \mu, \tau$) to the lightest mass eigenstates. From Eq. (2.8), it is clear that K is unitary if and only if $d_X^2 = 0$. Thus, the deviations from unitarity are manifestly expressed in the diagonal matrix d_X^2 containing the (squared) singular values of X .

In summary, a generic 6×6 mixing unitary matrix \mathcal{V} can be simplified and be written in terms of just one 3×3 unitary matrix V and of explicit deviations from unitarity, parametrised by a 3×3 matrix X :

$$\mathcal{V} = \begin{pmatrix} K & R \\ S & Z \end{pmatrix} \quad ; \quad \begin{aligned} K &= V \sqrt{(\mathbb{1} + X^\dagger X)^{-1}} & ; & \quad R = K X^\dagger, \\ Z &= \sqrt{(\mathbb{1} + X X^\dagger)^{-1}} & ; & \quad S = -Z X, \end{aligned} \quad (2.11)$$

i.e.

$$\mathcal{V} = \begin{pmatrix} V (\mathbb{1} + X^\dagger X)^{-1/2} & V (\mathbb{1} + X^\dagger X)^{-1/2} X^\dagger \\ -(\mathbb{1} + X X^\dagger)^{-1/2} X & (\mathbb{1} + X X^\dagger)^{-1/2} \end{pmatrix}. \quad (2.12)$$

In general, there are no restrictions on the matrix X . However, in a type-I seesaw model, the mixing matrix \mathcal{V} must also obey the mass relation stated in Eq. (2.3), and the 6×6 neutrino mass matrix \mathcal{M} is not general: some entries are zero at tree level. This imposes a restriction⁴ on X ,

$$d + X^T D X = 0, \quad (2.13)$$

which implies that it is possible to write X as:

$$X = i \sqrt{D^{-1}} O_c \sqrt{d}, \quad (2.14)$$

³Principal square roots of positive semi-definite matrices are unique and their use is implied in Eq. (2.8).

⁴This restriction generalises to $d + X^\dagger D X = K^{-1} m_L (K^{-1})^\dagger$ for an explicit, symmetric light neutrino Majorana mass matrix m_L in place of the zero in Eq. (2.2), which may arise from radiative corrections or be present due to e.g. a type-II seesaw [30–34] contribution.

	m_l	d	D	O_c	V	Total
Moduli	3	3	3	3	3	$15 = 9 + 6$
Phases	-3	0	0	3	6	6

Table 1: Physical parameter counting in type-I seesaw with three sterile neutrinos. The 15 moduli correspond to 9 lepton masses (3 charged-lepton masses and 6 neutrino masses) and to 6 mixing angles. There are 6 physical phases, as rephasing the charged leptons can remove 3 phases from V . Recall that m_l is real and diagonal in the considered weak basis.

where O_c is a complex orthogonal matrix, i.e., $O_c^T O_c = O_c O_c^T = \mathbb{1}$. Explicitly,

$$|X_{ij}| = \left| (O_c)_{ij} \sqrt{\frac{m_j}{M_i}} \right|. \quad (2.15)$$

Since O_c is an orthogonal complex matrix, not all of its elements need to be small. Furthermore, not all the M_i need to be much larger than the electroweak scale, in order for the seesaw mechanism to lead to naturally suppressed neutrino masses. These observations about the size of the elements of X are especially relevant in view of the fact that some of the important physical implications of the seesaw model depend crucially on X . In particular, the deviations of 3×3 unitarity are controlled by X , as shown in Eq. (2.8). On the other hand, from Eq. (2.13) one can also see that X must not vanish, in order to account for the non-zero light neutrino masses. Several authors have adopted different types of parametrisations for the full mixing matrix, in the context of seesaw models, see for example [35–39]. Some of these are approximate and apply to specific limits or to models with fewer than three sterile neutrinos, others are exact and do not depend on the number of sterile neutrinos like in our case.⁵ Some of these parametrisations were derived to deal with special types of analyses and may become cumbersome when adopted for other purposes. We find our parametrisation very useful since it is particularly simple and parametrises, in a concise and exact form, all deviations from unitarity by a single matrix X .

From the above, one concludes that the set $\{m_l, d, D, V, O_c\}$ of matrices is sufficient to describe lepton masses and mixing at tree level. In the working weak basis, there are 9 lepton masses in the first three matrices, while mixing is parametrised by 6 angles and 6 CP-violating (CPV) phases, contained in the unitary matrix V and in the orthogonal deviation matrix O_c . Parameter counting is summarised in Table 1 and is in agreement with, e.g., Refs. [40–42]. Coincidentally, these numbers of angles and CPV phases match those of a general 3+1 scenario (see e.g. [43]), even though three right-handed neutrinos have been added to the SM. This is a consequence of having a type-I seesaw UV completion, which requires the zero block in Eq. (2.2).

In this paper, we consider the possibility of having at least one sterile neutrino with a mass of order eV arising from the seesaw mechanism in a model with three right-handed neutrinos added to the SM. We analyse the different aspects and consequences of the phenomenology of such a model. With this aim, relations between observables and parameters which are independent of the seesaw limit are derived in the following subsection.

⁵ Although we have applied our parametrisation to a scenario with three sterile neutrinos, it is applicable to cases where the number q of sterile neutrinos differs from 3. We are then in the presence of a rectangular $3 \times q$ Dirac mass matrix m and of a $q \times 3$ rectangular X matrix, with everything else remaining consistent.

2.2 Exact Relations at Tree Level

From Eqs. (2.3) and (2.7), one can extract a general and exact formula for the neutrino Dirac mass matrix m in Eq. (2.2), valid for any weak basis and any scale of M :

$$m = KX^\dagger D (Z^{-1})^* = -iK\sqrt{d}O_c^\dagger\sqrt{D}(Z^{-1})^*. \quad (2.16)$$

Recall that, in our working weak basis, m_l is diagonal and K is directly identified with the non-unitary PMNS matrix. Moreover, K and Z take the forms given in Eq. (2.11) and one has:

$$\begin{aligned} m &= V\sqrt{(\mathbb{1} + X^\dagger X)^{-1}}X^\dagger D\sqrt{\mathbb{1} + X^*X^T} \\ &= -iV\sqrt{(\mathbb{1} + X^\dagger X)^{-1}}\sqrt{d}O_c^\dagger\sqrt{D}\sqrt{\mathbb{1} + X^*X^T}. \end{aligned} \quad (2.17)$$

This exact formula is to be contrasted with the known parametrisation for the neutrino Dirac mass matrix developed by Casas and Ibarra [44], which is valid in the standard seesaw limit of $M \gg m$ and reads

$$m \simeq -iU_{\text{PMNS}}\sqrt{d}O_c^{\text{CI}}\sqrt{D}, \quad (2.18)$$

in the weak basis where m_l and $M = \text{diag}(\tilde{M}_1, \tilde{M}_2, \tilde{M}_3) \equiv \tilde{D}$ are diagonal. Here, O_c^{CI} is an orthogonal complex matrix and U_{PMNS} represents the approximately unitary lepton mixing matrix. In this limit of $M \gg m$, the light neutrino mass matrix m_ν can be approximated by:

$$m_\nu \simeq -mM^{-1}m^T. \quad (2.19)$$

It is clear from (2.17) that one can obtain Eq. (2.18) as a limiting case of Eq. (2.16) through an expansion in powers of X . Keeping only the leading term, unitarity is regained with $U_{\text{PMNS}} \simeq V$ and one can identify the complex orthogonal matrices: $O_c^{\text{CI}} = O_c^\dagger$.

As a side note, let us remark that it is possible to obtain a parametrisation for m which is exact and holds in a general weak basis by following the Casas-Ibarra procedure. One finds:

$$m = -iU_\nu\sqrt{\tilde{d}}\tilde{O}_c^{\text{CI}}\sqrt{\tilde{D}}\Sigma_M^T, \quad (2.20)$$

where once again \tilde{O}_c^{CI} is a complex symmetric matrix. However, \tilde{d} and \tilde{D} do not contain physical masses, but are instead diagonal matrices with non-negative entries obtained from the Takagi decompositions $-mM^{-1}m = U_\nu\tilde{d}U_\nu^T$ and $M = \Sigma_M\tilde{D}\Sigma_M^T$, with U_ν and Σ_M unitary. The matrix Σ_M is unphysical, as it can be rotated away by a weak basis transformation diagonalising M . Even though this parametrisation resembles that of Eq. (2.17), the latter may be preferable since it directly makes use of low-energy observables. Only in the limit $M \gg m$, where Eq. (2.19) and $\tilde{d} \simeq d$, $\tilde{D} \simeq D$ hold, does Eq. (2.20) reduce to the approximate relation (2.18), in a weak basis of diagonal charged leptons and diagonal sterile neutrinos.

At this stage, one may wonder whether there exists an exact relation, analogous to Eq. (2.19) which is valid in any region of parameter space. One can actually deduce such a relation for an arbitrary number of active and sterile neutrinos. Consider the following decomposition of a block-diagonal matrix:

$$\begin{bmatrix} \mathbf{A} & \mathbf{B} \\ \mathbf{C} & \mathbf{D} \end{bmatrix} = \begin{bmatrix} \mathbb{1}_{(p \times p)} & \mathbf{B} \\ 0 & \mathbf{D} \end{bmatrix} \begin{bmatrix} \mathbf{A} - \mathbf{B}\mathbf{D}^{-1}\mathbf{C} & 0 \\ \mathbf{D}^{-1}\mathbf{C} & \mathbb{1}_{(q \times q)} \end{bmatrix}, \quad (2.21)$$

where \mathbf{A} , \mathbf{B} , \mathbf{C} , and \mathbf{D} are complex $p \times p$, $p \times q$, $q \times p$, and $q \times q$ matrices, respectively, and one has assumed that \mathbf{D} is non-singular. From this it follows that

$$\det \begin{bmatrix} \mathbf{A} & \mathbf{B} \\ \mathbf{C} & \mathbf{D} \end{bmatrix} = \det (\mathbf{A} - \mathbf{B}\mathbf{D}^{-1}\mathbf{C}) \det \mathbf{D}. \quad (2.22)$$

In a general type-I seesaw scenario, $\mathbf{A} = 0$, $\mathbf{B} = \mathbf{C}^T = m$ and $\mathbf{D} = M$, and one obtains

$$\left| \det \begin{bmatrix} 0 & m \\ m^T & M \end{bmatrix} \right| = |\det m|^2, \quad (2.23)$$

which leads to

$$m_1 \dots m_p = \frac{|\det m|^2}{M_1 \dots M_q}, \quad (2.24)$$

with m_i ($i = 1, \dots, p$) and M_j ($j = 1, \dots, q$) denoting the neutrino masses. For the case of interest, $p = q = 3$ and one has:

$$m_1 m_2 m_3 = \frac{|\det m|^2}{M_1 M_2 M_3}. \quad (2.25)$$

We stress that these relations are **exact** and that no assumptions have been made about the relative sizes of the m_i and M_j . It is clear from Eq. (2.25) that the smallness of neutrino masses in this framework may have its origin in the largeness of the M_j (with respect to the EW scale), or in the suppression of $|\det m|$ due to e.g. an approximate symmetry.

3 The Size of Deviations from Unitarity

Present neutrino experiments put stringent constraints on the deviations from unitarity [45–50]. In the framework of the type-I seesaw, it is the block \mathbf{K} of the matrix \mathcal{V} that takes the role played by the U_{PMNS} matrix at low energies, typically taken as unitary and parametrised accordingly (see e.g. the standard parametrisation [3]). Clearly, in this framework, \mathbf{K} is no longer a unitary matrix. When considering the deviations from unitarity of \mathbf{K} , one must comply with experimental bounds, while at the same time investigate whether it is possible to obtain deviations that are sizeable enough to be detected experimentally in the near future. Using the above parametrisation, this translates into making appropriate choices for the matrix \mathbf{X} . Deviations from unitarity of \mathbf{K} can be parametrised as the product of an Hermitian matrix by a unitary matrix [49]:

$$\mathbf{K} = (\mathbb{1} - \boldsymbol{\eta}) \mathbf{V}, \quad (3.1)$$

where $\boldsymbol{\eta}$ is an Hermitian matrix. In the previous section, we have instead parametrised \mathbf{K} with an Hermitian matrix to the right and the unitary matrix \mathbf{V} to the left, see Eq. (2.11). These right- and left-polar decompositions are unique since we are dealing with a non-singular \mathbf{K} by assumption. Moreover, they can be connected explicitly:

$$\boldsymbol{\eta} = \mathbf{V} \left(\mathbb{1} - \sqrt{(\mathbb{1} + \mathbf{X}^\dagger \mathbf{X})^{-1}} \right) \mathbf{V}^\dagger = \mathbb{1} - U_{\mathbf{K}} \left(\sqrt{\mathbb{1} + d_{\mathbf{X}}^2} \right)^{-1} U_{\mathbf{K}}^\dagger. \quad (3.2)$$

Expanding in powers of X (or equivalently of d_X), one obtains

$$\eta = \frac{1}{2} U_K d_X^2 U_K^\dagger + O(d_X^4) = \frac{1}{2} V X^\dagger X V^\dagger + O(X^4). \quad (3.3)$$

Constraints on the entries of η depend on the mass scale of the new neutrinos. Bounds on η can be found in the literature for the scenario in which all three heavier neutrinos have masses above the EW scale [48, 49]. As pointed out in [49], in such a case it is very useful to parametrise K with the unitary matrix on the right, due to the fact that, experimentally, it is not possible to determine which physical light neutrino is produced. Therefore, one must sum over the massive neutrino fields and observables depend on KK^\dagger . From the unitarity relation $KK^\dagger + RR^\dagger = \mathbb{1}$ and Eq. (3.1), one has

$$KK^\dagger = \mathbb{1} - RR^\dagger = \mathbb{1} - 2\eta + \eta^2 \quad \Rightarrow \quad \eta = \frac{1}{2} RR^\dagger + O(R^4), \quad (3.4)$$

i.e. there is a straightforward connection between KK^\dagger , RR^\dagger and the deviations from unitarity, expressed in η .

When one has one or more light sterile neutrinos, the aforementioned bounds cannot be directly applied, as some states are kinematically accessible and different sets of experimental constraints need to be taken into account, depending on the spectrum at hand. In this case, observables can constrain directly the entries of R , and not just the product RR^\dagger . For light sterile neutrinos with eV-scale masses, the most stringent bounds on deviations from unitarity come from oscillation experiments [50], such as BUGEY-3 [51], MINOS [52], NOMAD [53, 54] and Super-Kamiokande [55]. In our analysis, the relevant exclusion curves in the $\sin^2 2\vartheta_{\alpha\beta} - \Delta m^2$ planes (see section 5) are considered and translated into constraints on the elements of the mixing matrix block R . If one is dealing instead with keV or GeV–TeV sterile neutrinos, it is important to take into account the experimental bounds coming from β -decay experiments (see e.g. [56] and references within) and from LHC searches for heavy Majorana neutrinos [57–63]. Another crucial experimental input, also taken into account in our analysis, is the limit on the $\mu \rightarrow e\gamma$ branching ratio obtained by the MEG Collaboration, $BR(\mu \rightarrow e\gamma) < 4.2 \times 10^{-13}$ (90% CL) [64], one of the most stringent bounds on lepton flavour violating processes. This bound is expected to be relevant whenever the heavier neutrino masses are around or above the EW scale, as a GIM cancellation arises for lighter states (see for instance Eq. (40) of Ref. [49]).

3.1 Restrictions on the Neutrino Mass Spectrum

The type-I seesaw model that we consider here, with at least one sterile neutrino with a mass around 1 eV, also leads to some restrictions on the light neutrino mass spectrum at tree level. In particular, we find an upper bound on the mass m_{\min} of the lightest neutrino, as a function of the deviations from unitarity.

Taking into account the parametrisation (2.14) for the matrix X controlling deviations from unitarity, and for eigenvalues $d_{X_i}^2$ ($i = 1, 2, 3$) of $X^\dagger X$, we have:

$$\text{tr} [X^\dagger X] = \text{tr} [O_c^\dagger D^{-1} O_c d] = d_{X_1}^2 + d_{X_2}^2 + d_{X_3}^2. \quad (3.5)$$

From this, and recalling that $d = \text{diag}(m_1, m_2, m_3)$ and $D = \text{diag}(M_1, M_2, M_3)$, we obtain

$$\sum_k \frac{1}{M_k} \left(m_1 |O_{k1}^c|^2 + m_2 |O_{k2}^c|^2 + m_3 |O_{k3}^c|^2 \right) = d_{X_1}^2 + d_{X_2}^2 + d_{X_3}^2, \quad (3.6)$$

and conclude that

$$\frac{m_{\min}}{M_1} \left(|O_{11}^c|^2 + |O_{12}^c|^2 + |O_{13}^c|^2 \right) < d_{X_1}^2 + d_{X_2}^2 + d_{X_3}^2, \quad (3.7)$$

where naturally $M_1 \leq M_2 \leq M_3$ and $m_{\min} = m_1$ (m_3) for normal (inverted) ordering. Then, inserting the inequality $\sum_i |O_{1i}^c|^2 \geq 1$, valid for any orthogonal complex matrix, we find

$$m_{\min} < (d_{X_1}^2 + d_{X_2}^2 + d_{X_3}^2) M_1. \quad (3.8)$$

As discussed, when one has one or more light sterile neutrinos, the typical stringent conditions on the deviations from unitarity do not apply. Thus, one may consider larger deviations from unitarity, even of the order of the smallest U_{PMNS} angle, i.e. $O(0.1)$ [50]. Since in the scenarios of interest the lightest of the heaviest neutrinos has a mass of $M_1 \sim 1$ eV, using Eq. (3.8) we find a bound for the mass of the lightest neutrino:

$$m_{\min} \lesssim 0.1 \text{ eV}. \quad (3.9)$$

Note that this bound becomes stronger as one considers smaller and smaller deviations from unitarity. Taking into account the measured light neutrino mass-squared differences, we conclude that the light neutrinos cannot have masses above $O(0.1)$ eV under these conditions, a statement which is also supported by cosmological bounds [65].

3.2 Neutrino Oscillations

In the presence of deviations from unitarity, neutrino oscillation probabilities are modified [46, 50]. If n of the heavier neutrinos are accessible at oscillation experiments, then a $3 \times (3+n)$ submatrix Θ of \mathcal{V} enters the computation of oscillation probabilities,

$$\Theta = \begin{pmatrix} K & R_{3 \times n} \end{pmatrix}, \quad (3.10)$$

where $R_{3 \times n}$ contains the first n columns of R . For a given experimental setup, and depending on their masses, the heavier states may already be produced incoherently or instead lose coherence before reaching the detector, due to wave-packet separation (see e.g. [66]). The probability of transition between flavour (anti-)neutrinos $\bar{\nu}_\alpha$ and $\bar{\nu}_\beta$, or of survival for a given flavour ($\alpha = \beta$), with $\alpha, \beta = e, \mu, \tau$, can be shown to take the form

$$P_{\bar{\nu}_\alpha \rightarrow \bar{\nu}_\beta}(L, E) = \frac{1}{(\Theta \Theta^\dagger)_{\alpha\alpha} (\Theta \Theta^\dagger)_{\beta\beta}} \left[\left| (\Theta \Theta^\dagger)_{\alpha\beta} \right|^2 - 4 \sum_{i>j}^{3+n} \text{Re} \left(\Theta_{\alpha i}^* \Theta_{\beta i} \Theta_{\alpha j} \Theta_{\beta j}^* \right) \sin^2 \Delta_{ij} \right. \\ \left. \pm 2 \sum_{i>j}^{3+n} \text{Im} \left(\Theta_{\alpha i}^* \Theta_{\beta i} \Theta_{\alpha j} \Theta_{\beta j}^* \right) \sin 2\Delta_{ij} \right], \quad (3.11)$$

where the plus or minus sign in the second line refers to neutrinos or anti-neutrinos, respectively. Here, L denotes the source-detector distance, E is the (anti-)neutrino energy, and one has defined

$$\Delta_{ij} \equiv \frac{\Delta m_{ik}^2 L}{4E} \simeq 1.27 \frac{\Delta m_{ij}^2 [\text{eV}^2] L [\text{km}]}{E [\text{GeV}]}, \quad (3.12)$$

with mass-squared differences $\Delta m_{ij}^2 \equiv m_i^2 - m_j^2$, as usual.

Note that if $n = 3$ then $\Theta\Theta^\dagger = KK^\dagger + RR^\dagger = \mathbb{1}_{3 \times 3}$ due to the unitarity of the full 6×6 mixing matrix \mathcal{V} and Eq. (3.11) reduces to the usual unitary formula. It should be pointed out that the normalisation $(\Theta\Theta^\dagger)_{\alpha\alpha}(\Theta\Theta^\dagger)_{\beta\beta}$ in (3.11) will cancel in the experimental event rates, due to similar correction factors appearing in production rates and detection cross-sections [46, 66]. Nevertheless, we explicitly keep it in subsequent expressions. It will turn out to be negligibly close to unity for our particular numerical examples. The term proportional to $|(\Theta\Theta^\dagger)_{\alpha\beta}|^2$ is instead known to correspond to a “zero-distance” effect [46, 67]. It will also turn out to be negligible for our explicit numerical examples.

In what follows, we will consider approximate forms of Eq. (3.11), having in mind SBL and long-baseline (LBL) experimental setups. Since LBL experiments realistically need to take matter effects into account, our formulae in those cases are simply indicative.

4 Structure of the Mass Matrix

4.1 One-loop Corrections

So far we have focused on neutrino masses and mixing at tree level. However, in general, one expects one-loop corrections $\delta\mathcal{M}_L$ to the $0_{(3 \times 3)}$ block of \mathcal{M} in Eq. (2.2). As these are not guaranteed to be negligible, one should keep track of them in order to properly scan the parameter space of seesaw models. They are inherently finite and are given by [68, 69] (see also [70]):

$$\delta\mathcal{M}_L = \delta\mathcal{M}_L^Z + \delta\mathcal{M}_L^H, \quad (4.1)$$

where $\delta\mathcal{M}_L^Z$ and $\delta\mathcal{M}_L^H$ represent contributions depending on the Z and Higgs boson masses, m_Z and m_H , respectively. Explicitly, one has (see also Appendix A of Ref. [69]):

$$\begin{aligned} \delta\mathcal{M}_L^Z &= \frac{3}{32\pi^2 v^2} \begin{pmatrix} K & R \end{pmatrix} \frac{\mathcal{D}^3}{\mathcal{D}^2/m_Z^2 - \mathbb{1}} \log\left(\frac{\mathcal{D}^2}{m_Z^2}\right) \begin{pmatrix} K^T \\ R^T \end{pmatrix}, \\ \delta\mathcal{M}_L^H &= \frac{1}{32\pi^2 v^2} \begin{pmatrix} K & R \end{pmatrix} \frac{\mathcal{D}^3}{\mathcal{D}^2/m_H^2 - \mathbb{1}} \log\left(\frac{\mathcal{D}^2}{m_H^2}\right) \begin{pmatrix} K^T \\ R^T \end{pmatrix}, \end{aligned} \quad (4.2)$$

in a generic weak basis, with $v \simeq 174$ GeV being the Higgs VEV and with \mathcal{D} , K and R given in Eqs. (2.4) and (2.11). This result can be cast in a simple form:

$$\delta\mathcal{M}_L = K f(d) K^T + R f(D) R^T, \quad (4.3)$$

where naturally f is applied element-wise to diagonal matrices, with

$$f(m) \equiv \frac{m^3}{(4\pi v)^2} \left(\frac{3 \log(m/m_Z)}{m^2/m_Z^2 - 1} + \frac{\log(m/m_H)}{m^2/m_H^2 - 1} \right). \quad (4.4)$$

Models with very small deviations from unitarity (standard seesaw) have a very small X and hence a correspondingly small $R = KX^\dagger$. For these, the one-loop δM_L corrections are negligible, as can be seen from Eq. (4.3). Namely (aside from the loop-factor suppression), the terms with K are suppressed by the light neutrino masses d , whereas the effect of the heavier neutrino masses in D is regulated by the small entries of R . However, in models with sizeable deviations from unitarity, R is not small and controlling δM_L requires a mechanism such as a symmetry at the Lagrangian level.

4.2 Approximately Conserved Lepton Number

Relatively light sterile neutrinos can arise naturally in a seesaw framework in the presence of an approximately conserved lepton number [71–73]. Such a $U(1)_L$ symmetry, when exact, imposes specific textures on the mass matrices m and M . These textures may be slightly perturbed when the symmetry is approximate,⁶ allowing for non-vanishing Majorana neutrino masses and non-trivial mixing.

We are interested in scenarios where at least one of the mostly-sterile neutrinos is light, with a mass of $\mathcal{O}(\text{eV})$, in order to establish a connection to the SBL anomalies. We are further looking for situations where some of the Yukawa couplings are of order one. The choice of lepton charges should then be such that, in the exact conservation limit: i) M has zero determinant,⁷ and ii) not all entries of m are small. These conditions limit the possible $U(1)_L$ charge assignments.

The possibility of having a conserved (non-standard) lepton number has been considered in the past [28, 76, 77]. Following the analysis of Ref. [28], we work in a certain ‘symmetry’ weak basis in which lepton charge vectors λ_ν and λ_L are assigned to the three right-handed neutrino singlets and to the three lepton doublets, respectively. As anticipated in section 2.1, one generically has $\Sigma \neq 1$ in Eq. (2.10). Up to permutations, there are only 4 non-trivial choices of $U(1)_L$ charges leading to an M with zero determinant in the exact conservation limit: $\lambda_\nu = (1, 1, 0)$, $\lambda_\nu = (1, -1, -1)$, $\lambda_\nu = (1, 1, 1)$ and $\lambda_\nu = (0, 0, 1)$. Of these four, $\lambda_\nu = (1, 1, 1)$ is not viable as it imposes $M = 0$, and $\lambda_\nu = (0, 0, 1)$ is discarded since requiring controlled loop corrections in our framework effectively reduces it to the case with $\lambda_\nu = (1, -1, -1)$. We look into the remaining two options $\lambda_\nu = (1, 1, 0)$ and $\lambda_\nu = (1, -1, -1)$ in what follows. Given λ_ν , the choice of λ_L follows from the requirements that the seesaw mechanism is operative for all light neutrinos and that all left-handed neutrinos are allowed to couple to the right-handed ones [28].

⁶We allow for small perturbations to all entries of m and M , without any presumption regarding their origin. The case where only M departs from its symmetric texture, which manifestly corresponds to a soft breaking of the lepton number symmetry, was considered in Refs. [74, 75].

⁷In previous work [29], several cases were analysed following the $U(1)_L$ charge assignment $\lambda_\nu = (1, -1, 0)$ and $\lambda_L = (1, 1, 1)$, which however implies $\det M \neq 0$ in the symmetric limit.

4.2.1 Case I: $\lambda_v = (1, 1, 0)$

For this case, the only sensible choice for the doublet charges is $\lambda_L = (0, 0, 0)$. The mass matrices in the symmetric limit read:

$$m = \begin{pmatrix} 0 & 0 & a \\ 0 & 0 & b \\ 0 & 0 & c \end{pmatrix}, \quad M = \begin{pmatrix} 0 & 0 & 0 \\ 0 & 0 & 0 \\ 0 & 0 & M_3 \end{pmatrix}. \quad (4.5)$$

Breaking the symmetry will generate the light neutrino masses, two (mostly-)sterile states with masses M_1 and M_2 that can be much smaller than M_3 , and a heavy sterile with a mass close to M_3 . As expected, some Yukawa couplings remain of $\mathcal{O}(1)$, which can also be understood from Eq. (2.16), expressing the dependence of the Dirac mass matrix m on the sterile masses contained in D . This case is further separated into two subcases: one can allow for a hierarchy $M_2 \gg M_1$ (**case Ia**), which may arise in a scenario of stepwise symmetry breaking, or instead focus on a single new light-sterile scale, with $M_1 \sim M_2$ (**case Ib**).

4.2.2 Case II: $\lambda_v = (1, -1, -1)$

For this case, one is instead led to $\lambda_L = (1, 1, 1)$. In the exact conservation limit, the mass matrices are given by:

$$m = \begin{pmatrix} a & 0 & 0 \\ b & 0 & 0 \\ c & 0 & 0 \end{pmatrix}, \quad M = \begin{pmatrix} 0 & A & B \\ A & 0 & 0 \\ B & 0 & 0 \end{pmatrix}. \quad (4.6)$$

In this limit, one has two degenerate neutrinos with mass $\sqrt{|A|^2 + |B|^2}$ and opposite CP parities, forming a single heavy Dirac particle. Breaking the symmetry will allow for the generation of light neutrino masses and for another massive sterile state to arise, with a mass than can be much smaller than $|A|$ and $|B|$. It will additionally lift the mass degeneracy for the Dirac neutrino, producing a pseudo-Dirac neutrino pair [76, 78]. As pointed out in [79], a strong mass degeneracy translates into a symmetry in the R block of the mixing matrix, namely $R_{\alpha 2} \simeq \pm i R_{\alpha 3}$ ($\alpha = e, \mu, \tau$). Such a relation can be seen to play a fundamental role in suppressing the effect of the large masses M_2 and M_3 in the one-loop correction δM_L , see Eq. (4.3). It signals that one is close to the limit of lepton number conservation, even if $R_{\alpha 2}$ and $R_{\alpha 3}$ are not extremely suppressed.⁸ One is then allowed to have relatively large Yukawa couplings even if $M_2 \simeq M_3$ are not as large as the M_3 of case I. This can be seen from Eq. (2.16), which can be written in the form $m = R D (Z^{-1})^*$. The mass of the pseudo-Dirac pair can be at the TeV scale [73, 79–82], since the size of the lightest neutrino masses is protected by approximate lepton number conservation. The same symmetry and effects are present in the examples given in Ref. [29].

In the following section, we perform a numerical analysis focusing on cases Ia, Ib and II and incorporating an eV sterile neutrino in the seesaw spectrum while allowing for a mixing matrix K with sizeable deviations from unitarity.

⁸Nonetheless, it is true that in the exact conservation limit $d = X = R = 0$.

5 Numerical Analysis and Benchmarks

For each of the cases Ia, Ib and II defined in the previous section, we explicitly provide a numerical benchmark for the seesaw mass matrices, and explore the parameter space of qualitatively similar seesaw structures. As anticipated in section 3.2, we further provide approximate forms of the transition probabilities of muon to electron (anti-)neutrinos, $P_{\bar{\nu}_\mu \rightarrow \bar{\nu}_e}$, obtained from Eq. (3.11) while having in mind SBL and LBL setups, for each of the three scenarios. Given that recent global fits [83, 84] disfavour a light neutrino mass spectrum with inverted ordering (IO) with respect to one with normal ordering (NO) at more than the 3σ level, we restrict the mass ordering to NO in our numerical examples.

Before proceeding, note that the three scenarios of interest exhibit some correspondence to the commonly considered 3+1+1 (case Ia), 3+2 (case Ib), and 3+1 (case II) schemes, see for instance [20]. Thus, even though the connection to the latter is not exact – in particular, the spectrum of case Ib is not that of a typical 3+2 scenario – it may prove useful to consider quantities therein defined in our analysis, namely [85]

$$\sin^2 2\vartheta_{\mu e}^{(k)} \equiv 4 |\Theta_{\mu k}|^2 |\Theta_{ek}|^2, \quad (5.1)$$

with $k = 4$ in the 3+1 case, while $k = 4, 5$ for the other two cases. According to the global fit to SBL data of Ref. [85], explaining the observed anomalies requires $\Delta m_{41}^2 \in [0.87, 2.04] \text{ eV}^2$ and $\sin^2 2\vartheta_{\mu e}^{(4)} \in [6.5 \times 10^{-4}, 2.6 \times 10^{-3}]$ (99.7% CL) in the 3+1 scheme. This result may also be of relevance in the 3+1+1 scheme. Although we take these intervals as guidelines in our numerical explorations, it is not our aim to address the tensions in the current experimental situation of the SBL anomalies. Thus, we only restrict our sterile neutrino parameter space at the outset through the conservative bounds $\sum_i |R_{\alpha i}|^2 < 0.1$ ($\alpha = e, \mu, \tau$), and via the constraints of [53, 54, 56] on mixing matrix elements corresponding to large mass-squared differences $\Delta m^2 \sim 10 \text{ eV}^2 - 1 \text{ keV}^2$, as anticipated in section 3.

5.1 Case Ia: $M_1 \ll M_2 \ll M_3$

The numerical data for the benchmark corresponding to this case is given in Table 2a, where the one-loop correction of Eq. (4.3) has been taken into account. Apart from the three light mostly-active neutrinos, the spectrum includes three mostly-sterile neutrinos with masses $M_1 \sim 1 \text{ eV}$, $M_2 \sim 1 \text{ keV}$, and M_3 a few orders of magnitude below the grand unification (GUT) scale, $M_3 \sim 10^{14} \text{ GeV}$. The keV-scale neutrino may be a viable dark matter candidate [56, 86].

For the spectrum of case Ia, one has $n = 2$ in Eq. (3.10). In the context of a LBL experiment (e.g. DUNE [87]), the expression of Eq. (3.11) applied to the transition probability of muon to

Case Ia numerical benchmark			
m (GeV)	$\begin{bmatrix} (2.11 - 5.58i) \times 10^{-11} & (1.29 + 1.65i) \times 10^{-9} & 11.2 - 10.9i \\ (0.85 + 2.22i) \times 10^{-10} & (-5.29 + 3.99i) \times 10^{-9} & 10.4 + 0.4i \\ (-0.26 + 1.98i) \times 10^{-10} & (-4.51 - 1.05i) \times 10^{-9} & -10.5 - 34.6i \end{bmatrix}$		
M (GeV)	$\begin{bmatrix} 8.93 \times 10^{-10} & 4.45 \times 10^{-11} & 1.28 \times 10^{-13} \\ 4.45 \times 10^{-11} & 1.00 \times 10^{-6} & 6.22 \times 10^{-11} \\ 1.28 \times 10^{-13} & 6.22 \times 10^{-11} & 5.00 \times 10^{14} \end{bmatrix}$		
K	$\begin{bmatrix} -0.797 + 0.071i & 0.578 + 0.006i & -0.115 + 0.096i \\ 0.293 - 0.086i & 0.575 + 0.027i & 0.719 + 0.010i \\ -0.516 - 0.004i & -0.570 + 0.020i & 0.606 \end{bmatrix}$		
R	$\begin{bmatrix} 0.024 - 0.057i & (1.29 + 1.65i) \times 10^{-3} & (-2.24 + 2.18i) \times 10^{-14} \\ 0.093 + 0.223i & (-5.29 + 3.99i) \times 10^{-3} & (-2.08 + 0.08i) \times 10^{-14} \\ -0.026 + 0.199i & (-4.51 - 1.05i) \times 10^{-3} & (-2.10 + 6.92i) \times 10^{-14} \end{bmatrix}$		
X	$\begin{bmatrix} -0.003 - 0.015i & 0.102 + 0.023i & 0.050 - 0.317i \\ (-5.12 + 1.72i) \times 10^{-4} & (0.46 - 4.33i) \times 10^{-3} & (-7.30 - 2.18i) \times 10^{-3} \\ (0.23 + 5.33i) \times 10^{-14} & (-3.44 + 2.75i) \times 10^{-14} & (0.36 - 4.41i) \times 10^{-14} \end{bmatrix}$		
O_c (tree level)	$\begin{bmatrix} -0.53 + 0.12i & 0.22 - 1.12i & -1.41 - 0.22i \\ 0.22 + 0.56i & -1.50 - 0.13i & -0.30 + 1.03i \\ 1.00 - 0.06i & 0.23 + 0.25i & -0.14 - 0.01i \end{bmatrix}$		
Masses	$m_1 \simeq 1.06 \times 10^{-3} \text{ eV}, \quad m_2 \simeq 8.48 \times 10^{-3} \text{ eV}, \quad m_3 \simeq 5.02 \times 10^{-2} \text{ eV},$ $M_1 \simeq 1.00 \text{ eV}, \quad M_2 \simeq 1.00 \text{ keV}, \quad M_3 \simeq 5.00 \times 10^{14} \text{ GeV}$		
3v Δm^2	$\Delta m_{\odot}^2 = \Delta m_{21}^2 \simeq 7.08 \times 10^{-5} \text{ eV}^2, \quad \Delta m_{\text{atm}}^2 = \Delta m_{31}^2 \simeq 2.52 \times 10^{-3} \text{ eV}^2$		
3v mixing angles	$\sin^2 \theta_{12} \simeq 0.344, \quad \sin^2 \theta_{23} \simeq 0.585, \quad \sin^2 \theta_{13} \simeq 0.0236$		
3v CPV phases	$\delta \simeq 1.21\pi, \quad \alpha_{21} \simeq 0.06\pi, \quad \alpha_{31} \simeq 0.06\pi$		
$\sin^2 2\vartheta_{\mu e}^{(i)}$	$\sin^2 2\vartheta_{\mu e}^{(4)} \simeq 8.8 \times 10^{-4}, \quad \sin^2 2\vartheta_{\mu e}^{(5)} \simeq 7.7 \times 10^{-10}$		

Table 2a: Numerical benchmark for case Ia. The ordering of light neutrinos is NO. From the input matrices m and M , and taking into account one-loop corrections, the other quantities here listed follow. It should be noted that O_c of Eq. (2.14) is only defined at tree level. Values for the mixing angles and CPV phases of the 3v-framework in the standard parametrisation [3] are extracted by identifying the unitary matrix V with a unitary 3×3 PMNS mixing matrix.

electron (anti-)neutrinos can, in this case, be approximated by:

$$P_{\bar{\nu}_\mu \rightarrow \bar{\nu}_e}^{\text{LBL}} \simeq \frac{1}{(\Theta\Theta^\dagger)_{\mu\mu}(\Theta\Theta^\dagger)_{ee}} \left[\left| (\Theta\Theta^\dagger)_{\mu e} \right|^2 - 4 \sum_{i>j}^3 \text{Re}(\Theta_{\mu i}^* \Theta_{ei} \Theta_{\mu j} \Theta_{ej}^*) \sin^2 \Delta_{ij} \pm 2 \sum_{i>j}^3 \text{Im}(\Theta_{\mu i}^* \Theta_{ei} \Theta_{\mu j} \Theta_{ej}^*) \sin 2\Delta_{ij} - 4 \cdot \frac{1}{2} \text{Re} \left(\Theta_{\mu 4}^* \Theta_{e4} \sum_{j=1}^3 \Theta_{\mu j} \Theta_{ej}^* \right) - 4 \cdot \frac{1}{2} \text{Re} \left(\Theta_{\mu 5}^* \Theta_{e5} \sum_{j=1}^4 \Theta_{\mu j} \Theta_{ej}^* \right) \right], \quad (5.2)$$

where terms depending on $\Delta_{4j}, \Delta_{5j} \gg 1$ have been replaced by their averaged versions ($\sin^2 \Delta_{ij} \rightarrow 1/2, \sin 2\Delta_{ij} \rightarrow 0$). While the normalisation and the first term in this equation signal the loss of unitarity and a zero-distance effect, respectively, the last two terms explicitly represent the effects of the two lightest mostly-sterile states in oscillations. If one is in a condition similar to that of the numerical benchmark of Table 2a, for which $|(\Theta\Theta^\dagger)_{\mu\mu}(\Theta\Theta^\dagger)_{ee} - 1|$ and $|(\Theta\Theta^\dagger)_{\mu e}|^2$ are negligible, this expression can be further approximated by:

$$P_{\bar{\nu}_\mu \rightarrow \bar{\nu}_e}^{\text{LBL}} \simeq P_{\bar{\nu}_\mu \rightarrow \bar{\nu}_e}^{\text{LBL}, 3\nu} + \frac{1}{2} \sin^2 2\vartheta_{\mu e}^{(4)}, \quad (5.3)$$

where we have defined a 3ν -framework transition probability which, however, incorporates the effects of deviations of K from unitarity,

$$P_{\bar{\nu}_\mu \rightarrow \bar{\nu}_e}^{\text{LBL}, 3\nu} \equiv -4 \sum_{i>j}^3 \text{Re}(\Theta_{\mu i}^* \Theta_{ei} \Theta_{\mu j} \Theta_{ej}^*) \sin^2 \Delta_{ij} \pm 2 \sum_{i>j}^3 \text{Im}(\Theta_{\mu i}^* \Theta_{ei} \Theta_{\mu j} \Theta_{ej}^*) \sin 2\Delta_{ij}, \quad (5.4)$$

and have used the definition of Eq. (5.1), the unitarity of the full 6×6 mixing matrix, and the fact that $|\Theta_{\alpha 4}|^2 (= |R_{\alpha 1}|^2) \gg |\Theta_{\alpha 5}|^2 (= |R_{\alpha 2}|^2) \gg |R_{\alpha 3}|^2$.

In a SBL experiment (e.g. MicroBooNE [88]), the relevant form of Eq. (3.11) for $\bar{\nu}_\mu \rightarrow \bar{\nu}_e$ transitions is:

$$P_{\bar{\nu}_\mu \rightarrow \bar{\nu}_e}^{\text{SBL}} \simeq \frac{1}{(\Theta\Theta^\dagger)_{\mu\mu}(\Theta\Theta^\dagger)_{ee}} \left[\left| (\Theta\Theta^\dagger)_{\mu e} \right|^2 - 4 \cdot \frac{1}{2} \text{Re} \left(\Theta_{\mu 5}^* \Theta_{e5} \sum_{j=1}^4 \Theta_{\mu j} \Theta_{ej}^* \right) - 4 \text{Re} \left(\Theta_{\mu 4}^* \Theta_{e4} \sum_{j=1}^3 \Theta_{\mu j} \Theta_{ej}^* \right) \sin^2 \Delta_{41} \pm 2 \text{Im} \left(\Theta_{\mu 4}^* \Theta_{e4} \sum_{j=1}^3 \Theta_{\mu j} \Theta_{ej}^* \right) \sin 2\Delta_{41} \right], \quad (5.5)$$

with $\Delta_{41} \simeq \Delta_{42} \simeq \Delta_{43}$, and where terms depending on $\Delta_{5j} \gg 1$ have been replaced by their averaged versions ($\sin^2 \Delta_{5j} \rightarrow 1/2, \sin 2\Delta_{5j} \rightarrow 0$). In this context, one is sensitive to oscillations due to the scale of the mass-squared differences Δm_{4j}^2 with $j = 1, 2, 3$, while the oscillations pertaining to smaller mass-squared differences have not yet had a chance to develop. Finally, if one is in a condition similar to that of the numerical benchmark, this expression can be simply approximated by:

$$P_{\bar{\nu}_\mu \rightarrow \bar{\nu}_e}^{\text{SBL}} \simeq \sin^2 2\vartheta_{\mu e}^{(4)} \sin^2 \Delta_{41}, \quad (5.6)$$

where once again one has taken into account the unitarity of the full mixing matrix and the fact that $|R_{\alpha 1}|^2 \gg |R_{\alpha 2}|^2 \gg |R_{\alpha 3}|^2$.

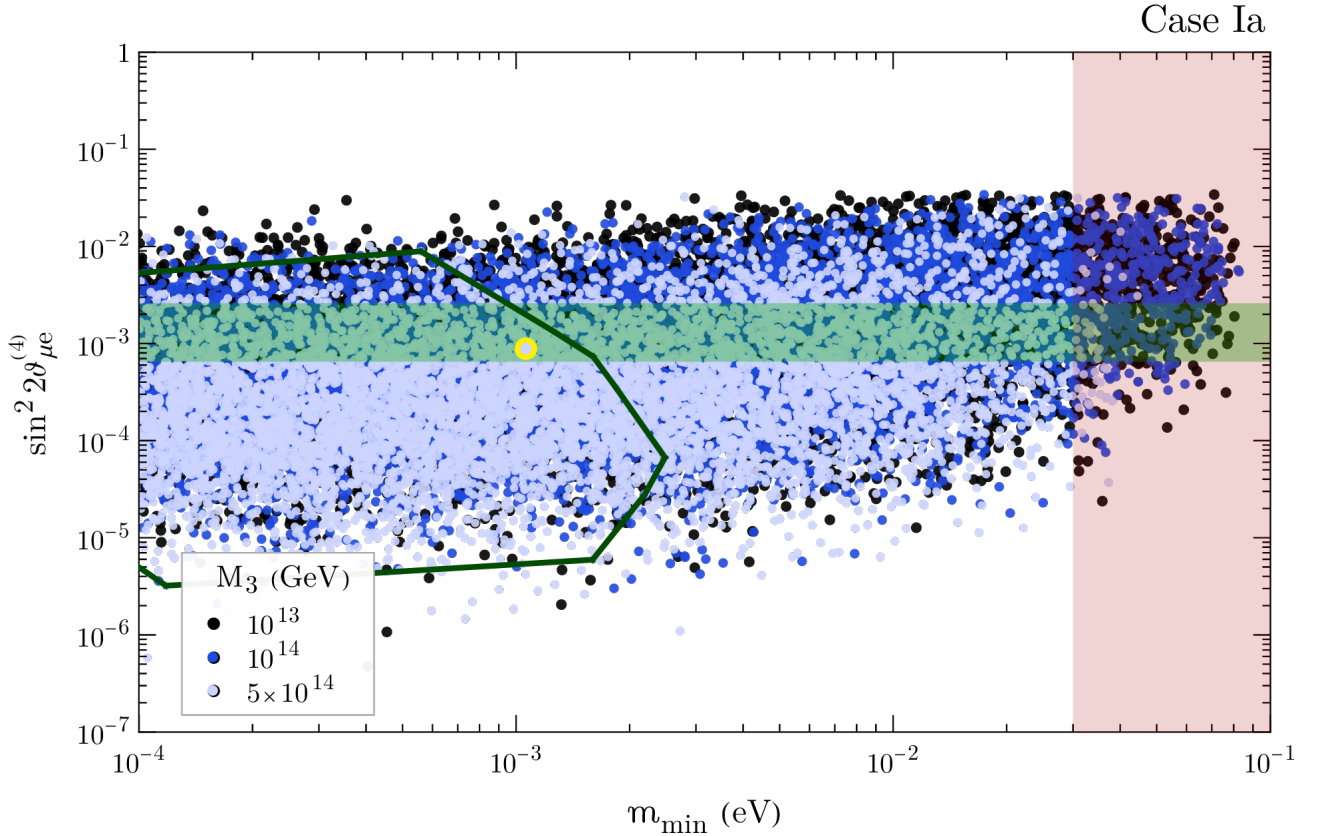


Figure 1: Active-sterile mixing measure $\sin^2 2\theta_{\mu e}^{(4)}$ versus the lightest neutrino mass m_{\min} from a scan of the case-Ia parameter space, with NO ($m_{\min} = m_1$). The heavy spectrum at tree level has $M_1 = 1$ eV and $M_2 = 1$ keV, while three values of the heaviest mass are considered, $M_3 = 10^{13} (10^{14}) [5 \times 10^{14}]$ GeV, corresponding to the black (dark blue) [light blue] points in the scatter plot. The horizontal green band shows the 99.7% CL interval of Ref. [85], while the vertical red exclusion band is obtained by combining the most stringent bound on the sum of light neutrino masses from cosmology, $\sum_i m_i < 0.12$ eV (95% CL) [89] [4], with the 3σ ranges of mass-squared differences. The dark green contour delimits the region inside which loop-stable points have been found (see text), while the benchmark of Table 2a is marked in yellow.

To further explore the parameter space of case Ia, we have produced numerical seesaw structures by specifying tree-level values of the unitary part V of the mixing matrix K , the mostly-active and mostly-sterile masses in d and D , and by scanning the complex orthogonal matrix O_c , parametrised as a product of three complex rotations times a sign corresponding to its determinant. We are interested in seesaw structures qualitatively similar to our benchmark, so that we specify (at tree level) $M_1 = 1$ eV and $M_2 = 1$ keV, while considering three different values for the heaviest neutrino mass, $M_3 \in \{10^{13}, 10^{14}, 5 \times 10^{14}\}$ GeV. While the lightest neutrino mass m_{\min} is scanned in the range $[10^{-4}, 0.1]$ eV, the remaining elements of d are fixed by specifying the solar and atmospheric mass differences. The 3ν mixing angles and Dirac CPV phase entering V as well as the aforementioned 3ν mass-squared differences are chosen to be the central values of the global fit of Ref. [84]. We stress that, as was the case for the numerical benchmark of Table 2a, 3ν mixing angles and CPV phases obtained while identifying V with a unitary 3×3 mixing matrix are expected to deviate slightly from the mixing angles and CPV phases arising in a parametrisation of the full 6×6 mixing matrix \mathcal{V} , due to deviations from unitarity. In

Figure 1 we show the values of $\sin^2 2\vartheta_{\mu e}^{(4)}$ in Eq. (5.1) against the values of the lightest neutrino mass, for the numerical examples found for case Ia. Only points for which $\text{tr}[mm^\dagger] \in [0.01, 1]v^2$ are kept.⁹ The horizontal green band highlights the range of $\sin^2 2\vartheta_{\mu e}^{(4)}$ preferred by the global fit of Ref. [85] and cited at the beginning of this section. The dark green contour instead delimits the region inside which relatively loop-stable points can be found, i.e. points which, after the one-loop correction of Eq. (4.3) has been implemented, still have 3ν mass-squared differences and mixing angles (extracted from V) inside the 3σ ranges of the fit [84]. From the figure it can be seen that raising the scale of M_3 will lower the scale of the light neutrino masses, disallowing too large values of m_{\min} . The approximations used in deriving the oscillation formulae of Eqs. (5.3) and (5.6) hold for all the plotted points.

Some quantities of potential phenomenological relevance, unrelated to neutrino oscillations, include the effective electron neutrino mass in β -decay, m_β , the absolute value of the effective neutrino Majorana mass controlling the rate of neutrinoless double beta $((\beta\beta)_{0\nu})$ -decay, $|m_{\beta\beta}|$, and the $\mu \rightarrow e\gamma$ branching ratio, $BR(\mu \rightarrow e\gamma)$. For all numerical examples pertaining to case Ia which are stable under loop corrections, the latter is unobservably small $BR(\mu \rightarrow e\gamma) \ll 10^{-30}$, while the former two are bounded by $m_\beta < 9.4$ meV and $|m_{\beta\beta}| < 6.7$ meV, and hence still out of reach of present and near-future experiments. In the computation of $|m_{\beta\beta}|$, the effects of the eV- and keV-scale neutrinos have been taken into account.

In the presence of a relatively large active-sterile mixing, future KATRIN-like experiments may be sensitive to the existence of sterile neutrinos with $O(\text{eV})$ masses [90]. This sensitivity is controlled by $|R_{e1}|^2 = |\mathcal{V}_{e4}|^2$, which is found to be bounded by $|R_{e4}|^2 \lesssim 0.02$ for the loop-stable numerical examples of this case. Sterile neutrinos with $O(\text{keV})$ masses may instead be detectable via kink-like signatures in next-generation β -decay experiments, even in the presence of small mixing $|R_{e2}|^2 = |\mathcal{V}_{e5}|^2 \sim 10^{-6}$ [91].

5.2 Case Ib: $M_1 \sim M_2 \ll M_3$

The numerical data for the benchmark corresponding to this case is given in Table 2b. Apart from the three light mostly-active neutrinos, the spectrum includes three mostly-sterile neutrinos with masses $M_1 \sim M_2 \sim 3$ eV, such that $M_2^2 - M_1^2 \simeq 1$ eV², while $M_3 \sim 10^{14}$ GeV.

For the spectrum of case Ib, one has $n = 2$ in Eq. (3.10). In a LBL context, the expression of Eq. (3.11) applied to the transition probability of muon to electron (anti-)neutrinos can be approximated by the same expression (5.2) given for case Ia. Once again, the last two terms in that equation explicitly show the effects of the two lightest mostly-sterile states in oscillations. If one is in a condition similar to that of the benchmark of Table 2b, for which $|(\Theta\Theta^\dagger)_{\mu\mu}(\Theta\Theta^\dagger)_{ee} - 1|$ and $|(\Theta\Theta^\dagger)_{\mu e}|^2$ are negligible, this expression can be further approximated by:

$$P_{\bar{\nu}_\mu \rightarrow \bar{\nu}_e}^{\text{LBL}} \simeq P_{\bar{\nu}_\mu \rightarrow \bar{\nu}_e}^{\text{LBL}, 3\nu} + \frac{1}{2} \left[\sin^2 2\vartheta_{\mu e}^{(4)} + \sin^2 2\vartheta_{\mu e}^{(5)} + 4 \text{Re}(\Theta_{\mu 4}^* \Theta_{e 4} \Theta_{\mu 5} \Theta_{e 5}^*) \right], \quad (5.7)$$

where we have used the unitarity of the full 6×6 mixing matrix, and the fact that $|R_{\alpha 1}|^2 \sim |R_{\alpha 2}|^2 \gg |R_{\alpha 3}|^2$. The latter prevents us from neglecting $|R_{\alpha 2}|^2$ (and hence $\sin^2 2\vartheta_{\mu e}^{(5)}$) with

⁹One may avoid very small Yukawa couplings by choosing appropriate values for M_3 and O_c .

Case Ib numerical benchmark			
m (GeV)	$\begin{bmatrix} (0.46 - 2.57i) \times 10^{-10} & (2.37 + 0.54i) \times 10^{-10} & 11.24 - 2.72i \\ (-5.50 - 1.04i) \times 10^{-10} & (0.68 - 6.20i) \times 10^{-10} & 8.90 - 27.50i \\ (-3.69 + 1.78i) \times 10^{-10} & (-1.60 - 4.45i) \times 10^{-10} & -1.85 + 0.43i \end{bmatrix}$		
M (GeV)	$\begin{bmatrix} 2.88 \times 10^{-9} & 8.24 \times 10^{-11} & 1.41 \times 10^{-11} \\ 8.24 \times 10^{-11} & 2.87 \times 10^{-9} & 1.42 \times 10^{-11} \\ 1.41 \times 10^{-11} & 1.42 \times 10^{-11} & 1.00 \times 10^{14} \end{bmatrix}$		
K	$\begin{bmatrix} -0.799 + 0.137i & 0.558 + 0.001i & 0.116 - 0.071i \\ 0.272 - 0.172i & 0.582 - 0.036i & -0.695 + 0.014i \\ -0.480 + 0.099i & -0.560 + 0.141i & -0.620 - 0.019i \end{bmatrix}$		
R	$\begin{bmatrix} 0.039 + 0.077i & 0.067 - 0.040i & (-1.12 + 0.27i) \times 10^{-13} \\ 0.156 - 0.105i & -0.097 - 0.170i & (-0.89 + 2.75i) \times 10^{-13} \\ 0.061 - 0.140i & -0.115 - 0.071i & (1.85 - 0.43i) \times 10^{-14} \end{bmatrix}$		
X	$\begin{bmatrix} -0.003 + 0.009i & 0.073 - 0.064i & -0.168 - 0.196i \\ -0.009 - 0.005i & 0.049 + 0.078i & 0.170 - 0.185i \\ (1.40 - 5.37i) \times 10^{-14} & (-1.47 - 1.74i) \times 10^{-13} & (0.37 + 2.24i) \times 10^{-13} \end{bmatrix}$		
O_c (tree level)	$\begin{bmatrix} -1.06 - 0.51i & -1.10 - 1.29i & -1.51 + 1.30i \\ 0.75 - 1.08i & 1.40 - 0.83i & -1.46 - 1.35i \\ 0.91 + 0.31i & -0.60 + 0.44i & 0.32 - 0.05i \end{bmatrix}$		
Masses	$m_1 \simeq 0.24 \times 10^{-3}$ eV,	$m_2 \simeq 8.76 \times 10^{-3}$ eV,	$m_3 \simeq 5.00 \times 10^{-2}$ eV,
	$M_1 \simeq 3.00$ eV,	$M_2 \simeq 3.16$ eV,	$M_3 \simeq 1.00 \times 10^{14}$ GeV
3v Δm^2	$\Delta m_{\odot}^2 = \Delta m_{21}^2 \simeq 7.66 \times 10^{-5}$ eV ² , $\Delta m_{\text{atm}}^2 = \Delta m_{31}^2 \simeq 2.50 \times 10^{-3}$ eV ²		
3v mixing angles	$\sin^2 \theta_{12} \simeq 0.327$, $\sin^2 \theta_{23} \simeq 0.562$, $\sin^2 \theta_{13} \simeq 0.0232$		
3v CPV phases	$\delta \simeq 1.26\pi$, $\alpha_{21} \simeq 0.11\pi$, $\alpha_{31} \simeq 0.22\pi$		
$\sin^2 2\vartheta_{\mu e}^{(i)}$	$\sin^2 2\vartheta_{\mu e}^{(4)} \simeq 1.1 \times 10^{-3}$, $\sin^2 2\vartheta_{\mu e}^{(5)} \simeq 9.2 \times 10^{-4}$		

Table 2b: The same as Table 2a for case Ib.

respect to $|R_{\alpha 1}|^2$ (and $\sin^2 2\vartheta_{\mu e}^{(4)}$), as we did in the previous case.

In a SBL context, the relevant form of Eq. (3.11) for $\bar{\nu}_\mu \rightarrow \bar{\nu}_e$ transitions in case Ib is:

$$P_{\bar{\nu}_\mu \rightarrow \bar{\nu}_e}^{\text{SBL}} \simeq \frac{1}{(\Theta\Theta^\dagger)_{\mu\mu}(\Theta\Theta^\dagger)_{ee}} \left[\left| (\Theta\Theta^\dagger)_{\mu e} \right|^2 - 4 \cdot \frac{1}{2} \text{Re} \left(\Theta_{\mu 4}^* \Theta_{e 4} \sum_{j=1}^3 \Theta_{\mu j} \Theta_{e j}^* \right) - 4 \cdot \frac{1}{2} \text{Re} \left(\Theta_{\mu 5}^* \Theta_{e 5} \sum_{j=1}^3 \Theta_{\mu j} \Theta_{e j}^* \right) - 4 \text{Re} \left(\Theta_{\mu 5}^* \Theta_{e 5} \Theta_{\mu 4} \Theta_{e 4}^* \right) \sin^2 \Delta_{54} \pm 2 \text{Im} \left(\Theta_{\mu 5}^* \Theta_{e 5} \Theta_{\mu 4} \Theta_{e 4}^* \right) \sin 2\Delta_{54} \right], \quad (5.8)$$

where terms depending on the large Δ_{4j} and Δ_{5j} ($j = 1, 2, 3$) have been replaced by their averaged versions. It is clear that this case does not correspond to a typical 3+2 scenario (see for instance [85]), since one has $\Delta m_{4j}^2, \Delta m_{5j}^2 \sim 10 \text{ eV}^2$ for $j = 1, 2, 3$. Hence, one can be sensitive to oscillations due to the mass-squared difference $\Delta m_{54}^2 \sim 1 \text{ eV}^2$, while oscillations pertaining to larger differences are averaged out and those driven by smaller mass-squared differences are underdeveloped. If one is in a condition similar to that of the numerical benchmark, this expression can be approximated by:

$$P_{\bar{\nu}_\mu \rightarrow \bar{\nu}_e}^{\text{SBL}} \simeq \frac{1}{2} \left(\sin^2 2\vartheta_{\mu e}^{(4)} + \sin^2 2\vartheta_{\mu e}^{(5)} \right) + 4 \text{Re} \left(\Theta_{\mu 4}^* \Theta_{e 4} \Theta_{\mu 5} \Theta_{e 5}^* \right) \cos^2 \Delta_{54} \mp 2 \text{Im} \left(\Theta_{\mu 4}^* \Theta_{e 4} \Theta_{\mu 5} \Theta_{e 5}^* \right) \sin 2\Delta_{54}, \quad (5.9)$$

where once again we have taken into account the unitarity of the full mixing matrix and the fact that $|R_{\alpha 1}|^2 \sim |R_{\alpha 2}|^2 \gg |R_{\alpha 3}|^2$. Notice that, unlike the typical 3+2 case, oscillations here depend on the square of the cosine of the relevant Δ_{ij} .

To further explore the parameter space of case Ib, we have produced numerical seesaw structures qualitatively similar to the benchmark by following the procedure described while discussing case Ia. We have specified (at tree level) $M_1 = 3.00 \text{ eV}$ and $M_2 = 3.16 \text{ eV}$, and have considered three different values for the heaviest neutrino mass, $M_3 \in \{10^{13}, 10^{14}, 5 \times 10^{14}\} \text{ GeV}$. In Figure 2 we show the values of the average of $\sin^2 2\vartheta_{\mu e}^{(4)}$ and $\sin^2 2\vartheta_{\mu e}^{(5)}$ against the values of the lightest neutrino mass, for the numerical examples found for case Ib. The former quantity is expected to represent the order of magnitude of potential signals of this case in SBL and LBL experiments. Only points for which $\text{tr} [mm^\dagger] \in [0.01, 1] v^2$ are kept. As before, the dark green contour delimits the region inside which relatively loop-stable points can be found. Raising the scale of M_3 will again lower the scale of the light neutrino masses. The approximations used in deriving the oscillation formulae of Eqs. (5.7) and (5.9) are valid for all the plotted points.

For all numerical examples pertaining to case Ib which are stable under loop corrections, $BR(\mu \rightarrow e\gamma) \ll 10^{-30}$ is unobservably small, while one finds $m_\beta < 9.3 \text{ meV}$ and $|m_{\beta\beta}| < 4.6 \text{ meV}$, still out of reach of present and near-future experiments. In the computation of $|m_{\beta\beta}|$, the effects of both eV-scale neutrinos have been taken into account. One additionally finds the bounds $|R_{e4}|^2, |R_{e5}|^2 \lesssim 0.01$ for the loop-stable numerical examples of this case.

Case II numerical benchmark			
m (GeV)	$\begin{bmatrix} -4.15 + 0.47i & (4.51 - 1.49i) \times 10^{-9} & (-1.59 + 0.13i) \times 10^{-9} \\ 3.98 + 6.17i & (-5.04 - 4.64i) \times 10^{-9} & (1.52 + 2.31i) \times 10^{-9} \\ 1.53 + 6.58i & (-1.90 - 2.68i) \times 10^{-9} & (0.59 + 2.59i) \times 10^{-9} \end{bmatrix}$		
M (GeV)	$\begin{bmatrix} 2.18 \times 10^{-6} & 1390 & 2.96 \\ 1390 & -2.19 \times 10^{-6} & 5.52 \times 10^{-7} \\ 2.96 & 5.52 \times 10^{-7} & 3.33 \times 10^{-9} \end{bmatrix}$		
K	$\begin{bmatrix} 0.825 + 0.061i & 0.536 + 0.027i & -0.092 + 0.108i \\ -0.302 + 0.113i & 0.581 - 0.017i & 0.728 - 0.052i \\ 0.455 + 0.054i & -0.599 + 0.075i & 0.651 + 0.002i \end{bmatrix}$		
R	$\begin{bmatrix} 0.063 - 0.056i & (2.11 - 0.24i) \times 10^{-3} & (-0.24 - 2.11i) \times 10^{-3} \\ -0.066 - 0.147i & (-2.03 - 3.13i) \times 10^{-3} & (-3.13 + 2.03i) \times 10^{-3} \\ -0.021 - 0.036i & (-0.79 - 3.35i) \times 10^{-3} & (-3.35 + 0.79i) \times 10^{-3} \end{bmatrix}$		
X	$\begin{bmatrix} 0.042 + 0.014i & 0.007 + 0.099i & -0.069 + 0.140i \\ (1.48 + 0.64i) \times 10^{-3} & (2.30 + 0.66i) \times 10^{-4} & (-2.11 + 4.89i) \times 10^{-3} \\ (-0.64 + 1.48i) \times 10^{-3} & (-0.66 + 2.30i) \times 10^{-4} & (-4.89 - 2.11i) \times 10^{-3} \end{bmatrix}$		
O_c (tree level)	$\begin{bmatrix} -0.21 + 0.62i & -1.02 + 0.06i & 0.62 + 0.31i \\ (-1.11 + 2.54i) \times 10^4 & (-1.05 + 2.42i) \times 10^3 & (2.55 + 1.12i) \times 10^4 \\ (-2.54 - 1.11i) \times 10^4 & (-2.42 - 1.05i) \times 10^3 & (-1.12 + 2.55i) \times 10^4 \end{bmatrix}$		
Masses	$m_1 \simeq 4.65 \times 10^{-3} \text{ eV}, \quad m_2 \simeq 9.47 \times 10^{-3} \text{ eV}, \quad m_3 \simeq 5.01 \times 10^{-2} \text{ eV},$ $M_1 \simeq 1.00 \text{ eV}, \quad M_2 \simeq 1390 \text{ GeV}, \quad M_3 \simeq 1390 \text{ GeV}$		
$3\nu \Delta m^2$	$\Delta m_{\odot}^2 = \Delta m_{21}^2 \simeq 6.80 \times 10^{-5} \text{ eV}^2, \quad \Delta m_{\text{atm}}^2 = \Delta m_{31}^2 \simeq 2.48 \times 10^{-3} \text{ eV}^2$		
3ν mixing angles	$\sin^2 \theta_{12} \simeq 0.298, \quad \sin^2 \theta_{23} \simeq 0.563, \quad \sin^2 \theta_{13} \simeq 0.0212$		
3ν CPV phases	$\delta \simeq 1.32\pi, \quad \alpha_{21} \simeq 1.99\pi, \quad \alpha_{31} \simeq 0.02\pi$		
$\sin^2 2\vartheta_{\mu e}^{(i)}$	$\sin^2 2\vartheta_{\mu e}^{(4)} \simeq 7.4 \times 10^{-4}$		

Table 2c: The same as Table 2a for case II. For this benchmark, $M_3 - M_2 \simeq 7.6 \text{ eV} \ll M_{2,3}$.

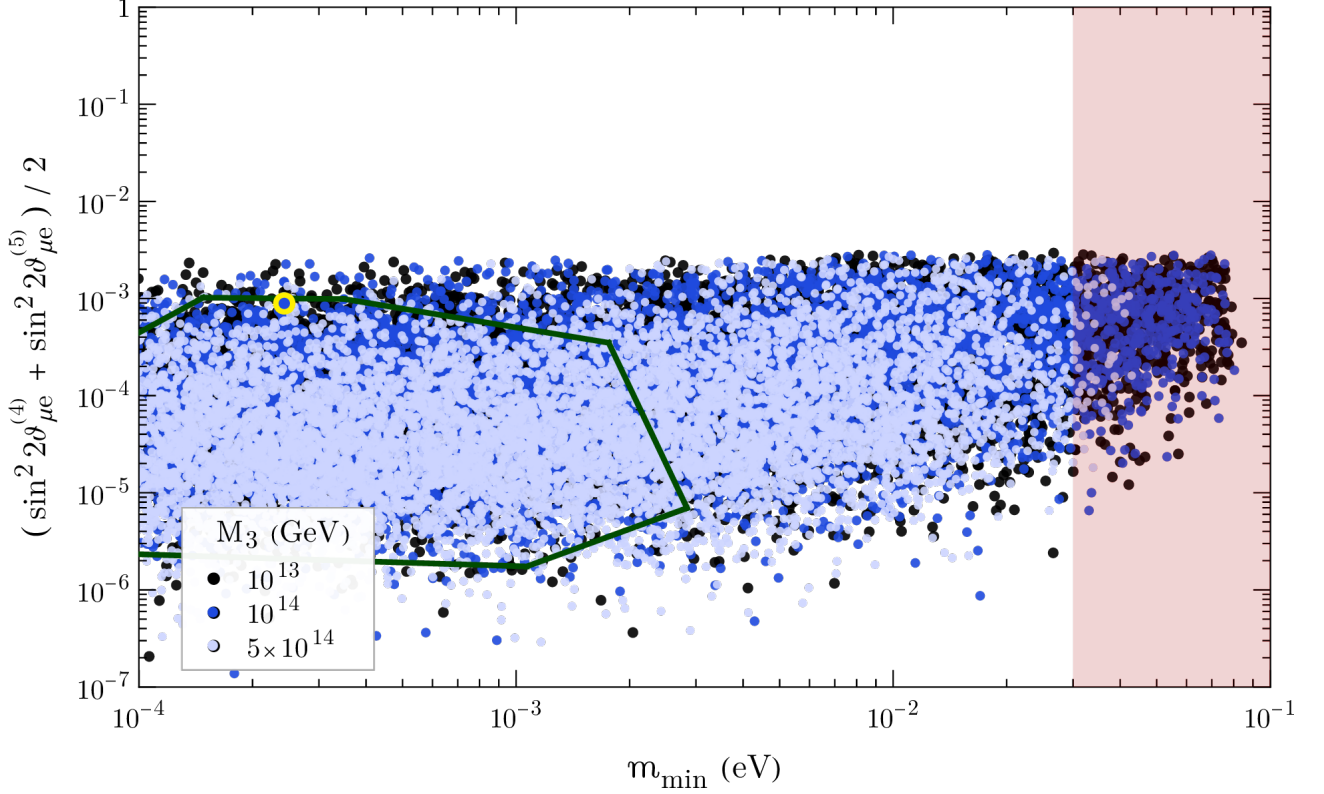


Figure 2: The average of $\sin^2 2\vartheta_{\mu e}^{(4)}$ and $\sin^2 2\vartheta_{\mu e}^{(5)}$ versus the lightest neutrino mass m_{\min} , from a scan of the case-Ib parameter space, with NO ($m_{\min} = m_1$). The heavy spectrum at tree level has $M_1 = 3.00$ eV and $M_2 = 3.16$ eV, while three values of the heaviest mass are considered, $M_3 = 10^{13} (10^{14}) [5 \times 10^{14}]$ GeV, corresponding to the black (dark blue) [light blue] points in the scatter plot. The vertical red band corresponds to the cosmological constraint, as in Figure 1. The dark green contour delimits the region inside which loop-stable points have been found, while the benchmark of Table 2b is marked in yellow.

5.3 Case II: $M_1 \ll M_2 \sim M_3$

The numerical data for the benchmark corresponding to this case is given in Table 2c. Apart from the three light mostly-active neutrinos, the spectrum includes a mostly-sterile neutrino with mass $M_1 \sim 1$ eV and a pair of quasi-degenerate neutrinos with masses $M_2 \simeq M_3 \sim 1$ TeV. From Table 2c one sees that the symmetry in the last two columns of R (recall section 4.2.2) is tied to an analogous symmetry in the last two rows of X and of O_c . The latter can be understood from Eqs. (2.11) and (2.14).

For the spectrum of case II, one has $n = 1$ in Eq. (3.10). In a LBL context, the expression of Eq. (3.11) applied to the transition probability of muon to electron (anti-)neutrinos can be

approximated by:

$$P_{\bar{\nu}_\mu \rightarrow \bar{\nu}_e}^{\text{LBL}} \simeq \frac{1}{(\Theta\Theta^\dagger)_{\mu\mu}(\Theta\Theta^\dagger)_{ee}} \left[\left| (\Theta\Theta^\dagger)_{\mu e} \right|^2 - 4 \cdot \frac{1}{2} \text{Re} \left(\Theta_{\mu 4}^* \Theta_{e 4} \sum_{j=1}^3 \Theta_{\mu j} \Theta_{e j}^* \right) \right. \\ \left. - 4 \sum_{i>j}^3 \text{Re} (\Theta_{\mu i}^* \Theta_{e i} \Theta_{\mu j} \Theta_{e j}^*) \sin^2 \Delta_{ij} \pm 2 \sum_{i>j}^3 \text{Im} (\Theta_{\mu i}^* \Theta_{e i} \Theta_{\mu j} \Theta_{e j}^*) \sin 2\Delta_{ij} \right], \quad (5.10)$$

where terms depending on $\Delta_{4j} \gg 1$ have been replaced by their averaged versions. If one is in a condition similar to that of the benchmark of Table 2c, for which $|(\Theta\Theta^\dagger)_{\mu\mu}(\Theta\Theta^\dagger)_{ee} - 1|$ and $|(\Theta\Theta^\dagger)_{\mu e}|^2$ are negligible, this expression can be further approximated by:

$$P_{\bar{\nu}_\mu \rightarrow \bar{\nu}_e}^{\text{LBL}} \simeq P_{\bar{\nu}_\mu \rightarrow \bar{\nu}_e}^{\text{LBL}, 3\nu} + \frac{1}{2} \sin^2 2\vartheta_{\mu e}^{(4)} + 4 \text{Re} (\Theta_{\mu 4}^* \Theta_{e 4} R_{\mu 2} R_{e 2}^*) . \quad (5.11)$$

Here, we have used the unitarity of the full 6×6 mixing matrix, and the approximate symmetry $R_{\alpha 2} \simeq i R_{\alpha 3}$. If, additionally $|\Theta_{\alpha 4}|^2 = |R_{\alpha 1}|^2 \gg |R_{\alpha 2}|^2 \simeq |R_{\alpha 3}|^2$, the last term can be neglected and one recovers Eq. (5.3) of case Ia.

In a SBL context, the relevant form of Eq. (3.11) for $\bar{\nu}_\mu \rightarrow \bar{\nu}_e$ transitions in case II is:

$$P_{\bar{\nu}_\mu \rightarrow \bar{\nu}_e}^{\text{SBL}} \simeq \frac{1}{(\Theta\Theta^\dagger)_{\mu\mu}(\Theta\Theta^\dagger)_{ee}} \left[\left| (\Theta\Theta^\dagger)_{\mu e} \right|^2 - 4 \text{Re} \left(\Theta_{\mu 4}^* \Theta_{e 4} \sum_{j=1}^3 \Theta_{\mu j} \Theta_{e j}^* \right) \sin^2 \Delta_{41} \right. \\ \left. \pm 2 \text{Im} \left(\Theta_{\mu 4}^* \Theta_{e 4} \sum_{j=1}^3 \Theta_{\mu j} \Theta_{e j}^* \right) \sin 2\Delta_{41} \right], \quad (5.12)$$

with $\Delta_{41} \simeq \Delta_{42} \simeq \Delta_{43}$. One is thus sensitive to oscillations due to the scale of mass-squared differences Δm_{4j}^2 with $j = 1, 2, 3$, while the oscillations pertaining to smaller mass-squared differences have not yet developed. If one is in a condition similar to that of the numerical benchmark, this expression can be approximated by:

$$P_{\bar{\nu}_\mu \rightarrow \bar{\nu}_e}^{\text{SBL}} \simeq \left[\sin^2 2\vartheta_{\mu e}^{(4)} + 8 \text{Re} (\Theta_{\mu 4}^* \Theta_{e 4} R_{\mu 2} R_{e 2}^*) \right] \sin^2 \Delta_{41} \mp 4 \text{Im} (\Theta_{\mu 4}^* \Theta_{e 4} R_{\mu 2} R_{e 2}^*) \sin 2\Delta_{41}, \quad (5.13)$$

where once again the unitarity of the full mixing matrix has been taken into account, as well as the relation $R_{\alpha 2} \simeq i R_{\alpha 3}$. If also $|R_{\alpha 1}|^2 \gg |R_{\alpha 2}|^2 \simeq |R_{\alpha 3}|^2$, then the two terms containing $R_{\alpha 2}$ in this equation can be neglected and one recovers Eq. (5.6) of case Ia.

To further explore the parameter space of case II, we have produced numerical seesaw structures qualitatively similar to our benchmark by following a procedure similar to that of case Ia. We have specified (at tree level) $M_1 = 1$ eV and three different values for the second heaviest neutrino mass, $M_2 (\simeq M_3) \in \{8, 14, 20\} \nu$, where $\nu \simeq 174$ GeV is the Higgs VEV. We have further scanned the mass splitting $M_3 - M_2$ in the interval $[0.02, 200]$ eV. In Figure 3 we show the values of $\sin^2 2\vartheta_{\mu e}^{(4)}$ in Eq. (5.1) against the values of the lightest neutrino mass, for the numerical examples found for case II. Only points for which $\text{tr} [mm^\dagger] \in [0.001, 1] \nu^2$ are kept. As before, the horizontal green band highlights the range of $\sin^2 2\vartheta_{\mu e}^{(4)}$ preferred by the global fit of Ref. [85] and cited at the beginning of the present section, while the dark green contour delimits the region inside which relatively loop-stable points can be found. The approximations

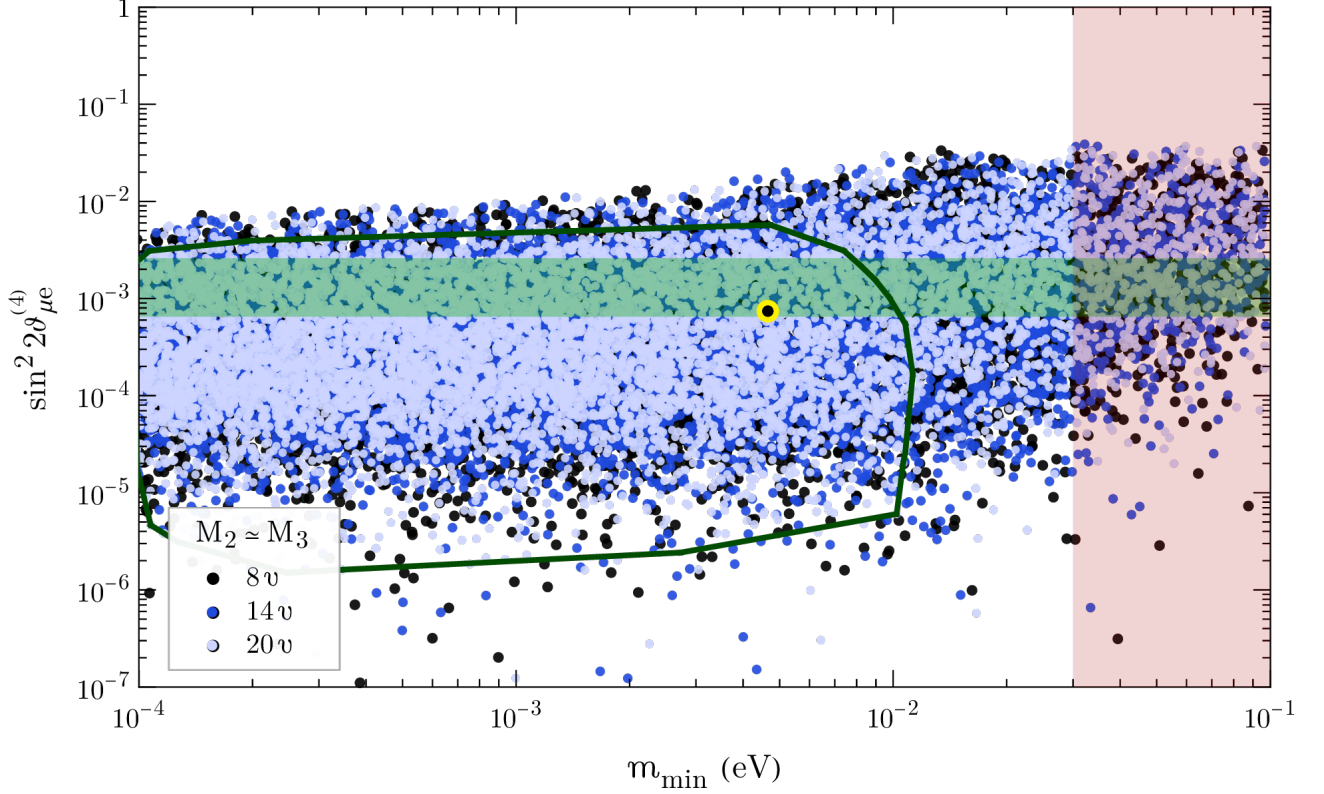


Figure 3: Active-sterile mixing measure $\sin^2 2\theta_{\mu e}^{(4)}$ versus the lightest neutrino mass m_{\min} from a scan of the case-II parameter space, with NO ($m_{\min} = m_1$). The heavy spectrum at tree level has $M_1 = 1$ eV, while three values of the heaviest quasi-degenerate masses are considered, $M_2 \simeq M_3 = 8\nu(14\nu)[20\nu]$, corresponding to the black (dark blue) [light blue] points in the scatter plot. Here, $\nu \simeq 174$ GeV is the Higgs VEV. The horizontal green band shows the 99.7% CL interval of Ref. [85], and the vertical red band corresponds to the cosmological constraint, as in Figure 1. The dark green contour delimits the region inside which loop-stable points have been found, while the benchmark of Table 2c is marked in yellow.

used in deriving the oscillation formulae of Eqs. (5.11) and (5.13) are valid for all the plotted points.

For the numerical examples pertaining to case II which are stable under loop corrections, one can obtain values of $BR(\mu \rightarrow e\gamma)$ close to the MEG upper bound of 4.2×10^{-13} . Points with larger values of the branching ratio are excluded from our scan. For the benchmark of Table 2c one has $BR(\mu \rightarrow e\gamma) \simeq 2.0 \times 10^{-13}$. Such effects can be probed by the MEG II update [92], which is expected to increase the present sensitivity of MEG by one order of magnitude. One also finds the bounds $m_\beta < 15$ meV, $|m_{\beta\beta}| < 27$ meV, and $|R_{e4}|^2 \lesssim 0.02$ for the loop-stable numerical examples of this case. While KATRIN will seek to improve the current bound on m_β down to 0.2 eV, values of $|m_{\beta\beta}| \gtrsim 10^{-2}$ eV may be probed in the next generation of $(\beta\beta)_{0\nu}$ -decay experiments [93]. Concerning the prospect of detecting the heavy neutrino pair in future collider searches, the reader is further referred to the review [94]. If, unlike our benchmark, the heavy neutrino pair would have a mass in the 1 – 100 GeV range and were sufficiently long-lived, it might lead to displaced vertex signatures [95] and produce resolvable neutrino-

antineutrino oscillations at colliders [96]. Finally, the pseudo-Dirac pair of case II might play a role in explaining the baryon asymmetry of the Universe through resonant leptogenesis [97]. In such a scenario, one should carefully take into account the washout from the interactions of the lighter sterile neutrino species.¹⁰ These interactions may need to be non-standard in order to reconcile the light sterile neutrino paradigm with cosmology.

The presented explicit numerical examples are merely illustrative. However, they give credit to our claim that models exhibiting an approximate lepton number symmetry with at least one sterile neutrino mass at the eV scale are viable and could play a part in explaining the SBL anomalies. In the next section we look into CP Violation in the present framework in some detail.

6 CP Violation in this Framework

6.1 Remarks on CP Violation Measurements

In order to analyse CP Violation effects, it is instructive to define CP asymmetries $A_{\nu\bar{\nu}}^{\alpha\beta}$ at the level of oscillation probabilities (see e.g. [99]):

$$A_{\nu\bar{\nu}}^{\alpha\beta} \equiv \frac{P_{\nu\alpha \rightarrow \nu\beta} - P_{\bar{\nu}\alpha \rightarrow \bar{\nu}\beta}}{P_{\nu\alpha \rightarrow \nu\beta} + P_{\bar{\nu}\alpha \rightarrow \bar{\nu}\beta}} \equiv \frac{\Delta P_{\alpha\beta}}{P_{\nu\alpha \rightarrow \nu\beta} + P_{\bar{\nu}\alpha \rightarrow \bar{\nu}\beta}}. \quad (6.1)$$

We restrict our discussion to the vacuum case, keeping in mind that in a realistic context the breaking of CP and CPT due to the asymmetry of the matter which neutrinos traverse should be taken into account. The requirement of CPT invariance results in the relations $\Delta P_{\alpha\beta} = -\Delta P_{\beta\alpha}$ and $\Delta P_{\alpha\alpha} = 0$. From the unitarity of the full mixing matrix, one further has

$$\sum_{\beta} \Delta P_{\alpha\beta} = 0, \quad (6.2)$$

for any α , with α and β running through the whole index set, $\alpha, \beta = e, \mu, \tau, s_1, \dots, s_q$. In a 3×3 unitary context, these relations imply that there is only one independent difference, which can be chosen as $\Delta P_{e\mu}$. As shown in [99], in a 4×4 unitary framework they imply the existence of 3 independent differences, say $\Delta P_{e\mu}$, $\Delta P_{\mu\tau}$, and $\Delta P_{\tau e}$. In the 6×6 unitary case, we find instead that there are 10 independent differences $\Delta P_{\alpha\beta}$ (see also [100]), while only the three of them involving just active neutrinos are experimentally relevant. Thus, one should generically expect different values for $\Delta P_{e\mu}$, $\Delta P_{\mu\tau}$, and $\Delta P_{\tau e}$ in a given seesaw-type model.

Using Eq. (3.11), with n mostly-sterile neutrinos accessible at an oscillation experiment, one finds:

$$\Delta P_{\alpha\beta} = \frac{4}{(\Theta\Theta^\dagger)_{\alpha\alpha}(\Theta\Theta^\dagger)_{\beta\beta}} \sum_{i>j}^{3+n} \text{Im} \left(\Theta_{\alpha i}^* \Theta_{\beta i} \Theta_{\alpha j} \Theta_{\beta j}^* \right) \sin 2\Delta_{ij}. \quad (6.3)$$

Even if none of the new sterile states are accessible – corresponding to $n = 0$ – one still expects $\Delta P_{e\mu}$, $\Delta P_{\mu\tau}$, and $\Delta P_{\tau e}$ to be independent, as the relevant 3×3 mixing submatrix $\Theta (= K)$ is not

¹⁰For an M_1 of case II in the range $[0.1, 50]$ keV, see the ISS(2,3) analysis of Ref. [98].

unitary. This means that it is possible for CP invariance to hold in one oscillation channel, such as $\bar{\nu}_\mu \rightarrow \bar{\nu}_e$ and yet be violated in another, such as $\bar{\nu}_\mu \rightarrow \bar{\nu}_\tau$. Indeed, one has:

$$\Delta P_{\mu\tau} = \Delta P_{e\mu} + \frac{4}{\prod_{\alpha=e,\mu,\tau}(\Theta\Theta^\dagger)_{\alpha\alpha}} \sum_{i>j}^3 \text{Im} \left[\Theta_{\mu i}^* \Theta_{\mu j} \left(\Theta_{ei} \Theta_{ej}^* (\Theta\Theta^\dagger)_{\tau\tau} + \Theta_{\tau i} \Theta_{\tau j}^* (\Theta\Theta^\dagger)_{ee} \right) \right] \sin 2\Delta_{ij}, \quad (6.4)$$

$$\Delta P_{\tau e} = \Delta P_{e\mu} - \frac{4}{\prod_{\alpha=e,\mu,\tau}(\Theta\Theta^\dagger)_{\alpha\alpha}} \sum_{i>j}^3 \text{Im} \left[\Theta_{ei}^* \Theta_{ej} \left(\Theta_{\mu i} \Theta_{\mu j}^* (\Theta\Theta^\dagger)_{\tau\tau} + \Theta_{\tau i} \Theta_{\tau j}^* (\Theta\Theta^\dagger)_{\mu\mu} \right) \right] \sin 2\Delta_{ij}. \quad (6.5)$$

It is then possible to have a zero $\Delta P_{e\mu}$ while $\Delta P_{\mu\tau}$ and/or $\Delta P_{\tau e}$ are non-zero. Notice that if Θ here were unitary, one would recover $\Delta P_{e\mu} = \Delta P_{\mu\tau} = \Delta P_{\tau e}$. Thus, deviations from unitarity are a potential source of CP Violation. This should come as no surprise, if one recalls that η in Eq. (3.1) is a complex hermitian matrix containing, in general, CPV physical phases.

For the cases analysed in sections 4 and 5, one has $n = 1, 2$. Explicit expressions for the CP asymmetries relevant in a SBL context can be obtained from the approximate relations (5.9) and (5.13) of cases Ib and II, respectively. Instead, from the relation (5.6) one sees that SBL CP asymmetries for case Ia are negligible. One has, for case Ib:

$$\Delta P_{e\mu}^{\text{SBL, Ib}} \simeq 4 \text{Im} \left(\Theta_{\mu 4}^* \Theta_{e 4} \Theta_{\mu 5} \Theta_{e 5}^* \right) \sin 2\Delta_{54}, \quad (6.6)$$

while for case II:

$$\Delta P_{e\mu}^{\text{SBL, II}} \simeq 8 \text{Im} \left(\Theta_{\mu 4}^* \Theta_{e 4} R_{\mu 2} R_{e 2}^* \right) \sin 2\Delta_{41}. \quad (6.7)$$

6.2 CP-odd Weak Basis Invariants

In section 2.1 we have shown (see also Ref. [40]) that in the present framework, where three right-handed neutrinos have been added to the SM, there are 6 CPV phases. They can be made to appear in the Dirac mass matrix m by changing to the weak basis (WB) where the charged lepton mass matrix m_l and the Majorana mass matrix M are diagonal and real. In the study of CP Violation, it is very useful to construct CP-odd WB invariants following the procedure introduced for the first time for the quark sector in Ref. [101], see also [102]. This procedure was later applied by different authors [40, 103–109] to the leptonic sector, in order to build CP-odd WB invariants relevant in several different contexts. Such invariants can be calculated in any convenient WB and their non-vanishing signals the presence of CP-breaking. We define six WB invariants which are sensitive to the leptonic CPV phases:

$$\begin{aligned} i_R &= \text{Im} \text{tr} \left[M^\dagger M m^\dagger m (M^\dagger M)^2 (m^\dagger m)^2 \right], & i_L &= \text{Im} \text{tr} \left[h_\ell m m^\dagger h_\ell^2 (m m^\dagger)^2 \right], \\ j_R^{(1)} &= \text{Im} \text{tr} \left[M^{-1} m^T m^* M m^\dagger m \right], & j_R^{(2)} &= \text{Im} \text{tr} \left[M^{-1} m^T m^* M (m^\dagger m)^2 \right], \\ j_L^{(1)} &= \text{Im} \text{tr} \left[M^\dagger M m^\dagger h_\ell m m^\dagger m \right], & j_L^{(2)} &= \text{Im} \text{tr} \left[M^\dagger M m^\dagger h_\ell m (m^\dagger m)^2 \right], \end{aligned} \quad (6.8)$$

where we have assumed M to be invertible and have additionally defined $h_\ell \equiv m_l m_l^\dagger$.

To see how the above invariants capture the 6 leptonic CPV phases, consider the aforementioned WB of m_l and M diagonal and real: $h_\ell = \text{diag}(m_e^2, m_\mu^2, m_\tau^2)$ and $M = \tilde{D} = \text{diag}(\tilde{M}_1, \tilde{M}_2, \tilde{M}_3)$. Recall that in this basis the full neutrino mass matrix \mathcal{M} is not diagonal and therefore the \tilde{M}_i do not coincide with the physical masses M_i . We further consider the singular value decomposition of m :

$$m = V_L d_m V_R, \quad (6.9)$$

with $V_{L,R}$ unitary and $d_m = \text{diag}(d_1, d_2, d_3)$ real and positive. The 6 physical CPV phases of interest are contained in m , since 3 out of its original 9 can be removed by rephasing left-handed fields. A parametrisation of V_L and V_R which captures explicitly these phases is:

$$V_L = V_{\delta_L} K_L, \quad V_R = V_{\delta_R} K_R, \quad (6.10)$$

with $K_{L,R} \equiv \text{diag}(1, e^{i\alpha_{L,R}}, e^{i\beta_{L,R}})$ and

$$V_{\delta_{L,R}} \equiv O_{23} \text{diag}(1, 1, e^{i\delta_{L,R}}) O_{13} O_{12}, \quad (6.11)$$

the O_{ij} being ordinary real rotation matrices in the i - j plane, e.g.

$$O_{23}(\theta_{23L}) = \begin{pmatrix} 1 & 0 & 0 \\ 0 & \cos \theta_{23L} & \sin \theta_{23L} \\ 0 & -\sin \theta_{23L} & \cos \theta_{23L} \end{pmatrix}. \quad (6.12)$$

The phases of interest are then manifestly $\alpha_{L,R}$, $\beta_{L,R}$ and $\delta_{L,R}$. Using this parametrisation, the invariants can be cast in the forms:

$$\begin{aligned} i_R &= \mathcal{K}_{i_R} \sin \delta_R, \quad i_L = \mathcal{K}_{i_L} \sin \delta_L, \\ j_R^{(a)} &= \mathcal{K}_{j_R^{(a)}}^{\delta_R} \sin \delta_R + \mathcal{K}_{j_R^{(a)}}^{2\alpha_R} \sin 2\alpha_R + \mathcal{K}_{j_R^{(a)}}^{2\beta_R} \sin 2\beta_R, \\ j_L^{(a)} &= \mathcal{K}_{j_L^{(a)}}^{\delta_R} \sin \delta_R + \mathcal{K}_{j_L^{(a)}}^{\delta_L} \sin \delta_L + \mathcal{K}_{j_L^{(a)}}^{\alpha_L} \sin \alpha_L + \mathcal{K}_{j_L^{(a)}}^{\beta_L} \sin \beta_L, \end{aligned} \quad (6.13)$$

with $a = 1, 2$. Explicit expressions for the \mathcal{K} coefficients are given in Appendix A. It is clear that i_R and i_L are sensitive to CPV values of δ_R and δ_L , respectively, while the $j_R^{(1,2)}$ ($j_L^{(1,2)}$) are further sensitive to α_R and β_R (α_L and β_L).

7 Summary and Conclusions

We have seen that in the framework of the type-I seesaw mechanism one can naturally have at least one sterile neutrino with a mass of around one eV. This can be inferred using a general exact parametrisation, defined in [29], that is valid irrespectively of the size and structure of the neutrino mass matrix. Thus we are able to analyse a general seesaw where not all of the three mostly-sterile neutrinos need to be very heavy. We have focused on models where at least one of the sterile neutrinos is light and its mixing with the active neutrinos is small enough to respect experimental bounds but sufficiently large to be relevant to low energy phenomenology – for instance, providing a natural explanation to the short-baseline anomalies.

In section 2, we have shown how the usual seesaw formulae have to be generalised in order to be applicable to the special region of parameters which we are considering. In particular, we have written the full neutrino mixing matrix in terms of a 3×3 unitary matrix and a 3×3 general complex matrix, which encodes the deviations from unitarity. The latter was further parametrised at tree level in terms of neutrino masses and a complex orthogonal matrix. We carefully distinguish approximate and exact relations, which are valid in any seesaw regime. Namely, we have found an exact formula for the neutrino Dirac mass matrix m in terms of neutrino masses, neutrino mixing and deviations from unitarity, which generalises the usual Casas-Ibarra parametrisation of m . We additionally derive an exact seesaw-like relation, equating the product of neutrino masses and the square of the absolute value of $\det m$.

In section 3, we have further discussed the parametrisation of deviations from unitarity as well as constraints on said deviations in our framework. These significantly depend on the masses of the heavy neutrinos. In this context, we also find a bound on the lightest neutrino mass m_{\min} , useful whenever a light sterile is present in the seesaw spectrum. For the cases of interest, with an eV-scale sterile neutrino and large deviations from unitarity, one has $m_{\min} \lesssim 0.1$ eV.

In sections 4 and 5 we give examples of viable textures with at least one sterile neutrino with a mass at the eV scale. Such light sterile states arise naturally by imposing an approximately conserved lepton number symmetry. Before the breaking, and for an appropriate assignment of leptonic charges, the lightest neutrinos are massless at tree level. After the breaking, the lightest neutrinos acquire calculable masses, with mass differences in agreement with experiment, after the relevant one-loop correction to the zero block of the neutrino mass matrix has been taken into account. This correction is cast in a simple form, highlighting the cancellations required by radiative stability, in section 4.1. We identify two symmetric textures (I and II) of the neutrino mass matrix which allow for a separation of high (TeV – GUT) and low (\lesssim keV) scales. We then concentrate on three particular scenarios, with differing spectra (M_1, M_2, M_3) of heavy neutrinos: case Ia, for which $M_1 \ll M_2 \ll M_3$; case Ib, with $M_1 \sim M_2 \ll M_3$; and case II, where $M_1 \ll M_2 \sim M_3$. Numerical benchmarks are given for each of these three cases in Tables 2a – 2c. Related regions in parameter space are explored in Figures 1 – 3, which show that these models can accommodate enough active-sterile mixing to play a role in the explanation of short-baseline anomalies. Since the formulae for neutrino oscillation probabilities are modified in the presence of deviations from unitarity, we present, for each case, approximate expressions for muon to electron (anti-)neutrino transition probabilities, quantifying the impact of light sterile states on oscillations, for both short- and long-baseline experiments. Attention is further given to the future testability of the proposed models through non-oscillation effects of the extra neutrino states.

We conclude our work in section 6 by discussing CP Violation in the type-I seesaw framework under analysis. At the level of oscillation probability asymmetries, we have found that deviations from unitarity may source CP Violation, with generically independent effects in the standard transition channels. We have also constructed 6 CP-odd weak basis invariants which are sensitive to the CP-violating phases in the lepton sector. This last point has been shown explicitly, for a particular choice of weak basis and parametrisation of m .

Acknowledgements

This work was supported by Fundação para a Ciência e a Tecnologia (FCT, Portugal) through the projects CFTP-FCT Unit 777 (UID/FIS/00777/2013 and UID/FIS/00777/2019), CERN/FIS-PAR/0004/2017, and PTDC/FIS-PAR/29436/2017 which are partially funded through POCTI (FEDER), COMPETE, QREN and EU. The work of PMFP was supported by several short term Master-type fellowships from the CFTP and CERN projects listed above. At present PMFP acknowledges support from FCT through PhD grant SFRH/BD/145399/2019. The work of JTP has been supported by the PTDC project listed above. GCB and MNR thank the CERN Theoretical Physics Department, where part of this work was done, for hospitality and partial support and also acknowledge participation in the CERN Neutrino Platform – Theory working group (CENF-TH).

A Explicit Expressions for Weak Basis Invariants

Using the definitions of section 6.2, and in the WB there considered, the WB invariants of Eq. (6.8) read:

$$\begin{aligned} i_R &= \frac{1}{2i} \sum_{ijkl} \tilde{M}_i^2 \tilde{M}_k^4 d_j^2 d_l^2 (d_l^2 - d_j^2) (V_{\delta_R})_{jk} (V_{\delta_R})_{li} (V_{\delta_R})_{ji}^* (V_{\delta_R})_{lk}^* \\ &= \frac{1}{2i} \sum_{ijkl} \tilde{M}_i^2 \tilde{M}_k^2 (\tilde{M}_k^2 - \tilde{M}_i^2) d_j^2 d_l^4 (V_{\delta_R})_{jk} (V_{\delta_R})_{li} (V_{\delta_R})_{ji}^* (V_{\delta_R})_{lk}^* , \end{aligned} \quad (\text{A.1})$$

$$\begin{aligned} i_L &= \frac{1}{2i} \sum_{ijkl} (h_\ell)_l (h_\ell)_j^2 d_i^2 d_k^2 (d_k^2 - d_i^2) (V_{\delta_L})_{jk} (V_{\delta_L})_{li} (V_{\delta_L})_{ji}^* (V_{\delta_L})_{lk}^* \\ &= \frac{1}{2i} \sum_{ijkl} (h_\ell)_j (h_\ell)_l [(h_\ell)_j - (h_\ell)_l] d_i^2 d_k^4 (V_{\delta_L})_{jk} (V_{\delta_L})_{li} (V_{\delta_L})_{ji}^* (V_{\delta_L})_{lk}^* , \end{aligned} \quad (\text{A.2})$$

$$j_R^{(1)} = \frac{1}{2i} \sum_{ijkl} d_i^2 d_k^2 \frac{\tilde{M}_l^2 - \tilde{M}_j^2}{\tilde{M}_l \tilde{M}_j} (K_R)_j^2 (K_R)_l^* (V_{\delta_R})_{ij} (V_{\delta_R})_{kj} (V_{\delta_R})_{il}^* (V_{\delta_R})_{kl}^* , \quad (\text{A.3})$$

$$j_R^{(2)} = \frac{1}{2i} \sum_{ijkl} d_i^4 d_k^2 \frac{\tilde{M}_l^2 - \tilde{M}_j^2}{\tilde{M}_l \tilde{M}_j} (K_R)_j^2 (K_R)_l^* (V_{\delta_R})_{ij} (V_{\delta_R})_{kj} (V_{\delta_R})_{il}^* (V_{\delta_R})_{kl}^* , \quad (\text{A.4})$$

$$j_L^{(1)} = \frac{1}{2i} \sum_{ijkl} d_i d_k (d_i^2 - d_k^2) \tilde{M}_j^2 (h_\ell)_l (K_L)_i (K_L)_k^* (V_{\delta_R})_{ij} (V_{\delta_R})_{kj}^* (V_{\delta_L})_{li} (V_{\delta_L})_{lk}^* , \quad (\text{A.5})$$

$$j_L^{(2)} = \frac{1}{2i} \sum_{ijkl} d_i d_k (d_i^4 - d_k^4) \tilde{M}_j^2 (h_\ell)_l (K_L)_i (K_L)_k^* (V_{\delta_R})_{ij} (V_{\delta_R})_{kj}^* (V_{\delta_L})_{li} (V_{\delta_L})_{lk}^* . \quad (\text{A.6})$$

Using further the given parametrisations of $V_{\delta_{L,R}}$ and $K_{L,R}$, one obtains the result of Eq. (6.13), with:

$$\begin{aligned} \mathcal{K}_R &= -\frac{1}{8} \cos \theta_{13R} \sin 2\theta_{12R} \sin 2\theta_{13R} \sin 2\theta_{23R} \\ &\quad \times (d_1^2 - d_2^2) (d_2^2 - d_3^2) (d_3^2 - d_1^2) (\tilde{M}_1^2 - \tilde{M}_2^2) (\tilde{M}_2^2 - \tilde{M}_3^2) (\tilde{M}_3^2 - \tilde{M}_1^2) , \end{aligned} \quad (\text{A.7})$$

$$\mathcal{K}_L = \frac{1}{8} \cos \theta_{13L} \sin 2\theta_{12L} \sin 2\theta_{13L} \sin 2\theta_{23L} \times (d_1^2 - d_2^2) (d_2^2 - d_3^2) (d_3^2 - d_1^2) (m_e^2 - m_\mu^2) (m_\mu^2 - m_\tau^2) (m_\tau^2 - m_e^2), \quad (\text{A.8})$$

$$\begin{aligned} \mathcal{K}_{j_R^{(a)}}^{\delta_R} &= \Delta_2^{(a)} \cos 2\alpha_R \cos 2\beta_R + 2\Delta_3^{(a)} \cos 2\alpha_R \cos 2\beta_R \cos \delta_R \\ &\quad - \Delta_6^{(a)} \frac{8 \cos 2\theta_{12R}}{\cos 4\theta_{12R} + 3} \cos 2\alpha_R \cos \delta_R - \Delta_7^{(a)} \frac{\cos 2\alpha_R}{\cos 2\theta_{12R}} \\ &\quad + \Delta_8^{(a)} \cos 2\beta_R + 2\Delta_9^{(a)} \cos 2\beta_R \cos \delta_R, \end{aligned} \quad (\text{A.9})$$

$$\begin{aligned} \mathcal{K}_{j_R^{(a)}}^{2\alpha_R} &= -\Delta_2^{(a)} \cos(2\beta_R + \delta_R) - \Delta_3^{(a)} \cos 2(\beta_R + \delta_R) + \Delta_4^{(a)} \cos 2\beta_R + \Delta_5^{(a)} \\ &\quad + \Delta_6^{(a)} \cos \delta_R + \Delta_7^{(a)} \cos 2\delta_R, \end{aligned} \quad (\text{A.10})$$

$$\begin{aligned} \mathcal{K}_{j_R^{(a)}}^{2\beta_R} &= \Delta_1^{(a)} + \Delta_2^{(a)} \cos 2\alpha_R \cos \delta_R + \Delta_3^{(a)} \cos 2\alpha_R \cos 2\delta_R - \Delta_4^{(a)} \cos 2\alpha_R \\ &\quad + \Delta_8^{(a)} \cos \delta_R + \Delta_9^{(a)} \cos 2\delta_R, \end{aligned} \quad (\text{A.11})$$

$$\begin{aligned} \mathcal{K}_{j_L^{(a)}}^{\delta_R} &= \Delta_3'^{(a)} \cos(\alpha_L - \beta_L) + \Delta_4'^{(a)} \cos 2\theta_{12L} \cos \delta_L \cos \alpha_L - \Delta_5'^{(a)} \cos \beta_L \cos \delta_L \\ &\quad + \Delta_9'^{(a)} \cos \alpha_L - \Delta_{10}'^{(a)} \frac{\cos(\alpha_L - \beta_L - \delta_L)}{\cos 2\theta_{23R}} + \Delta_{12}'^{(a)} \cos \beta_L, \end{aligned} \quad (\text{A.12})$$

$$\begin{aligned} \mathcal{K}_{j_L^{(a)}}^{\delta_L} &= \Delta_2'^{(a)} \cos \alpha_L \cos \beta_L - \Delta_4'^{(a)} \cos(\alpha_L + \delta_R) - \Delta_5'^{(a)} \cos \beta_L \cos \delta_R \\ &\quad - \Delta_7'^{(a)} \frac{\cos \alpha_L}{\cos 2\theta_{12L}} - \Delta_{10}'^{(a)} \cos \delta_R \cos \alpha_L \cos \beta_L + \Delta_{11}'^{(a)} \cos \beta_L, \end{aligned} \quad (\text{A.13})$$

$$\begin{aligned} \mathcal{K}_{j_L^{(a)}}^{\alpha_L} &= -\Delta_2'^{(a)} \cos(\beta_L + \delta_L) - \Delta_3'^{(a)} \cos 2\theta_{23R} \cos \delta_R \cos \beta_L \\ &\quad + \Delta_4'^{(a)} \cos 2\theta_{12L} \cos \delta_L \cos \delta_R + \Delta_6'^{(a)} \cos \beta_L + \Delta_7'^{(a)} \cos \delta_L + \Delta_8'^{(a)} \\ &\quad + \Delta_9'^{(a)} \cos \delta_R + \Delta_{10}'^{(a)} \cos \delta_R \cos(\beta_L + \delta_L), \end{aligned} \quad (\text{A.14})$$

$$\begin{aligned} \mathcal{K}_{j_L^{(a)}}^{\beta_L} &= \Delta_1'^{(a)} \sin \beta_L + \Delta_2'^{(a)} \cos \alpha_L \cos \delta_L + \Delta_3'^{(a)} \cos 2\theta_{23R} \cos \delta_R \cos \alpha_L \\ &\quad - \Delta_5'^{(a)} \cos(\delta_L + \delta_R) - \Delta_6'^{(a)} \cos \alpha_L - \Delta_{10}'^{(a)} \cos \delta_R \cos \alpha_L \cos \delta_L \\ &\quad + \Delta_{11}'^{(a)} \cos \delta_L + \Delta_{12}'^{(a)} \cos \delta_R. \end{aligned} \quad (\text{A.15})$$

It should be noted that the $\Delta_i^{(a)}$, where $a = 1, 2$, are independent of the 6 leptonic CPV phases $\delta_{R,L}$, $\alpha_{R,L}$, and $\beta_{R,L}$. The rather lengthy expressions for these quantities are finally given below:

$$\begin{aligned} \Delta_1^{(1)} &= \frac{1}{16} \frac{\tilde{M}_1^2 - \tilde{M}_3^2}{\tilde{M}_1 \tilde{M}_3} \cos^2 \theta_{12R} \sin^2 \theta_{13R} [(d_1^2 - d_2^2) + (d_1^2 - d_3^2) + \cos 2\theta_{23R} (d_2^2 - d_3^2)]^2, \\ \Delta_2^{(1)} &= \frac{1}{8} \frac{\tilde{M}_2^2 - \tilde{M}_3^2}{\tilde{M}_2 \tilde{M}_3} \cos \theta_{13R} \sin 2\theta_{13R} \sin 2\theta_{23R} \sin 2\theta_{12R} (d_2^2 - d_3^2) \\ &\quad \times [(d_1^2 - d_2^2) + (d_1^2 - d_3^2) + \cos 2\theta_{23R} (d_2^2 - d_3^2)], \end{aligned}$$

$$\begin{aligned}
\Delta_3^{(1)} &= \frac{1}{4} \frac{\tilde{M}_2^2 - \tilde{M}_3^2}{\tilde{M}_2 \tilde{M}_3} \cos^2 \theta_{13R} \cos^2 \theta_{12R} \sin^2 2\theta_{23R} (d_2^2 - d_3^2)^2, \\
\Delta_4^{(1)} &= -\frac{1}{16} \frac{\tilde{M}_2^2 - \tilde{M}_3^2}{\tilde{M}_2 \tilde{M}_3} \sin^2 \theta_{12R} \sin^2 2\theta_{13R} [(d_1^2 - d_2^2) + (d_1^2 - d_3^2) + \cos 2\theta_{23R} (d_2^2 - d_3^2)]^2, \\
\Delta_5^{(1)} &= \frac{1}{128} \frac{\tilde{M}_1^2 - \tilde{M}_2^2}{\tilde{M}_1 \tilde{M}_2} \sin^2 2\theta_{12R} \\
&\quad \times \left[12 (d_1^2 - d_2^2) (d_1^2 - d_3^2) - 5 (d_2^2 - d_3^2)^2 \right. \\
&\quad \quad + \cos 2\theta_{23R} (d_2^2 - d_3^2) [27 \cos 2\theta_{23R} (d_2^2 - d_3^2) - 10 ((d_1^2 - d_2^2) + (d_1^2 - d_3^2))] \\
&\quad \quad + 2 \cos 2\theta_{13R} ((d_2^2 - d_3^2)^2 + 8 (d_1^2 - d_2^2) (d_1^2 - d_3^2) - 5 \cos 4\theta_{23R} (d_2^2 - d_3^2)^2 \\
&\quad \quad \quad \left. - 4 \cos 2\theta_{23R} ((d_1^2 - d_2^2) + (d_1^2 - d_3^2)) (d_2^2 - d_3^2) \right) \\
&\quad \quad \left. + \cos 4\theta_{13R} ((d_1^2 - d_2^2) + (d_1^2 - d_3^2) + \cos 2\theta_{23R} (d_2^2 - d_3^2))^2 \right], \\
\Delta_6^{(1)} &= \frac{1}{16} \frac{\tilde{M}_1^2 - \tilde{M}_2^2}{\tilde{M}_1 \tilde{M}_2} \sin 4\theta_{12R} \sin \theta_{13R} \sin 2\theta_{23R} (d_2^2 - d_3^2) \\
&\quad \times [(3 - \cos 2\theta_{13R}) \cos 2\theta_{23R} (d_2^2 - d_3^2) - 2 \cos^2 \theta_{13R} ((d_1^2 - d_2^2) + (d_1^2 - d_3^2))], \\
\Delta_7^{(1)} &= \frac{1}{16} \frac{\tilde{M}_1^2 - \tilde{M}_2^2}{\tilde{M}_1 \tilde{M}_2} (3 + \cos 4\theta_{12R}) \sin^2 \theta_{13R} \sin^2 2\theta_{23R} (d_2^2 - d_3^2)^2, \\
\Delta_8^{(1)} &= -\frac{1}{8} \frac{\tilde{M}_1^2 - \tilde{M}_3^2}{\tilde{M}_1 \tilde{M}_3} \cos \theta_{13R} \sin 2\theta_{13R} \sin 2\theta_{23R} \sin 2\theta_{12R} (d_2^2 - d_3^2) \\
&\quad \times [(d_1^2 - d_2^2) + (d_1^2 - d_3^2) + \cos 2\theta_{23R} (d_2^2 - d_3^2)], \\
\Delta_9^{(1)} &= \frac{1}{4} \frac{\tilde{M}_1^2 - \tilde{M}_3^2}{\tilde{M}_1 \tilde{M}_3} \cos^2 \theta_{13R} \sin^2 \theta_{12R} \sin^2 2\theta_{23R} (d_2^2 - d_3^2)^2.
\end{aligned}$$

$$\begin{aligned}
\Delta_1^{(2)} &= \frac{1}{16} \frac{\tilde{M}_1^2 - \tilde{M}_3^2}{\tilde{M}_1 \tilde{M}_3} \cos^2 \theta_{12R} \sin^2 \theta_{13R} \\
&\quad \times [(d_1^2 - d_2^2) + (d_1^2 - d_3^2) + \cos 2\theta_{23R} (d_2^2 - d_3^2)] \\
&\quad \times [(d_1^4 - d_2^4) + (d_1^4 - d_3^4) + \cos 2\theta_{23R} (d_2^4 - d_3^4)], \\
\Delta_2^{(2)} &= \frac{1}{8} \frac{\tilde{M}_2^2 - \tilde{M}_3^2}{\tilde{M}_2 \tilde{M}_3} \cos \theta_{13R} \sin 2\theta_{13R} \sin 2\theta_{23R} \sin 2\theta_{12R} (d_2^2 - d_3^2) \\
&\quad \times [(d_1^4 - d_2^4) + (d_1^4 - d_3^4) - (d_1^2 - d_2^2) (d_1^2 - d_3^2) + \cos 2\theta_{23R} (d_2^4 - d_3^4)], \\
\Delta_3^{(2)} &= \frac{1}{4} \frac{\tilde{M}_2^2 - \tilde{M}_3^2}{\tilde{M}_2 \tilde{M}_3} \cos^2 \theta_{13R} \cos^2 \theta_{12R} \sin^2 2\theta_{23R} (d_2^2 - d_3^2) (d_2^4 - d_3^4), \\
\Delta_4^{(2)} &= -\frac{1}{16} \frac{\tilde{M}_2^2 - \tilde{M}_3^2}{\tilde{M}_2 \tilde{M}_3} \sin^2 \theta_{12R} \sin^2 2\theta_{13R} \\
&\quad \times [(d_1^2 - d_2^2) + (d_1^2 - d_3^2) + \cos 2\theta_{23R} (d_2^2 - d_3^2)] \\
&\quad \times [(d_1^4 - d_2^4) + (d_1^4 - d_3^4) + \cos 2\theta_{23R} (d_2^4 - d_3^4)], \\
\Delta_5^{(2)} &= \frac{1}{256} \frac{\tilde{M}_1^2 - \tilde{M}_2^2}{\tilde{M}_1 \tilde{M}_2} \sin^2 2\theta_{12R}
\end{aligned}$$

$$\begin{aligned}
& \times [12 ((d_1^2 - d_2^2) (d_1^4 - d_2^4) + (d_1^2 - d_3^2) (d_1^4 - d_3^4)) + 5 (d_2^2 - d_3^2) (d_2^4 - d_3^4) \\
& + 27 \cos 4\theta_{23R} (d_2^2 - d_3^2) (d_2^4 - d_3^4) \\
& + 20 \cos 2\theta_{23R} ((d_1^2 - d_2^2) (d_1^4 - d_2^4) - (d_1^2 - d_3^2) (d_1^4 - d_3^4)) \\
& + 4 \cos 2\theta_{13R} (4 [(d_1^2 - d_2^2) (d_1^4 - d_2^4) + (d_1^2 - d_3^2) (d_1^4 - d_3^4) \\
& + \cos 2\theta_{23R} ((d_1^2 - d_2^2) (d_1^4 - d_2^4) - (d_1^2 - d_3^2) (d_1^4 - d_3^4))] \\
& - (3 + 5 \cos 4\theta_{23R}) (d_2^2 - d_3^2) (d_2^4 - d_3^4)) \\
& + 2 \cos 4\theta_{13R} (2 [\cos 2\theta_{23R} ((d_1^2 - d_3^2) (d_1^4 - d_3^4) - (d_1^2 - d_2^2) (d_1^4 - d_2^4)) \\
& + (d_1^2 - d_2^2) (d_1^4 - d_2^4) + (d_1^2 - d_3^2) (d_1^4 - d_3^4)] \\
& - \sin^2 2\theta_{23R} (d_2^2 - d_3^2) (d_2^4 - d_3^4))] , \\
\Delta_6^{(2)} &= \frac{1}{16} \frac{\tilde{M}_1^2 - \tilde{M}_2^2}{\tilde{M}_1 \tilde{M}_2} \sin 4\theta_{12R} \sin \theta_{13R} \sin 2\theta_{23R} (d_2^2 - d_3^2) \\
& \times [(3 - \cos 2\theta_{13R}) \cos 2\theta_{23R} (d_2^4 - d_3^4) \\
& - 2 \cos^2 \theta_{13R} ((d_1^4 - d_2^4) + (d_1^4 - d_3^4) - (d_1^2 - d_2^2) (d_1^2 - d_3^2))] , \\
\Delta_7^{(2)} &= \frac{1}{16} \frac{\tilde{M}_1^2 - \tilde{M}_2^2}{\tilde{M}_1 \tilde{M}_2} (3 + \cos 4\theta_{12R}) \sin^2 \theta_{13R} \sin^2 2\theta_{23R} (d_2^2 - d_3^2) (d_2^4 - d_3^4) , \\
\Delta_8^{(2)} &= -\frac{1}{8} \frac{\tilde{M}_1^2 - \tilde{M}_3^2}{\tilde{M}_1 \tilde{M}_3} \cos \theta_{13R} \sin 2\theta_{13R} \sin 2\theta_{23R} \sin 2\theta_{12R} (d_2^2 - d_3^2) \\
& \times [(d_1^4 - d_2^4) + (d_1^4 - d_3^4) - (d_1^2 - d_2^2) (d_1^2 - d_3^2) + \cos 2\theta_{23R} (d_2^4 - d_3^4)] , \\
\Delta_9^{(2)} &= \frac{1}{4} \frac{\tilde{M}_1^2 - \tilde{M}_3^2}{\tilde{M}_1 \tilde{M}_3} \cos^2 \theta_{13R} \sin^2 \theta_{12R} \sin^2 2\theta_{23R} (d_2^2 - d_3^2) (d_2^4 - d_3^4) .
\end{aligned}$$

$$\begin{aligned}
\Delta_1'^{(a)} &= -\frac{1}{8} d_1 d_3 (d_1^{2a} - d_3^{2a}) \cos \theta_{12L} \sin 2\theta_{13L} \cos \theta_{13R} \sin 2\theta_{12R} \sin \theta_{23R} \\
& \times [(m_e^2 - m_\mu^2) + (m_e^2 - m_\tau^2) + \cos 2\theta_{23L} (m_\mu^2 - m_\tau^2)] (\tilde{M}_1^2 - \tilde{M}_2^2) , \\
\Delta_2'^{(a)} &= \frac{1}{16} d_2 d_3 (d_2^{2a} - d_3^{2a}) \cos \theta_{12L} \cos \theta_{13L} \sin 2\theta_{23L} \sin 2\theta_{23R} \\
& \times [2 \cos^2 \theta_{13R} ((\tilde{M}_1^2 - \tilde{M}_3^2) + (\tilde{M}_2^2 - \tilde{M}_3^2)) \\
& - \cos 2\theta_{12R} (3 - \cos 2\theta_{13R}) (\tilde{M}_1^2 - \tilde{M}_2^2)] (m_\mu^2 - m_\tau^2) , \\
\Delta_3'^{(a)} &= -\frac{1}{8} d_2 d_3 (d_2^{2a} - d_3^{2a}) \sin \theta_{12L} \sin 2\theta_{13L} \sin 2\theta_{12R} \sin \theta_{13R} \\
& \times [(m_e^2 - m_\mu^2) + (m_e^2 - m_\tau^2) + \cos 2\theta_{23L} (m_\mu^2 - m_\tau^2)] (\tilde{M}_1^2 - \tilde{M}_2^2) , \\
\Delta_4'^{(a)} &= -\frac{1}{8} d_1 d_2 (d_1^{2a} - d_2^{2a}) \sin \theta_{13L} \sin 2\theta_{23L} \sin 2\theta_{13R} \sin \theta_{23R} \\
& \times [(\tilde{M}_1^2 - \tilde{M}_3^2) + (\tilde{M}_2^2 - \tilde{M}_3^2) + \cos 2\theta_{12R} (\tilde{M}_1^2 - \tilde{M}_2^2)] (m_\mu^2 - m_\tau^2) , \\
\Delta_5'^{(a)} &= \frac{1}{8} d_1 d_3 (d_1^{2a} - d_3^{2a}) \cos \theta_{13L} \sin \theta_{12L} \sin 2\theta_{23L} \cos \theta_{23R} \sin 2\theta_{13R} \\
& \times [(\tilde{M}_1^2 - \tilde{M}_3^2) + (\tilde{M}_2^2 - \tilde{M}_3^2) + \cos 2\theta_{12R} (\tilde{M}_1^2 - \tilde{M}_2^2)] (m_\mu^2 - m_\tau^2) , \\
\Delta_6'^{(a)} &= -\frac{1}{32} d_2 d_3 (d_2^{2a} - d_3^{2a}) \sin \theta_{12L} \sin 2\theta_{13L} \sin 2\theta_{23R}
\end{aligned}$$

$$\begin{aligned}
& \times [2 \cos^2 \theta_{13R} ((\tilde{M}_1^2 - \tilde{M}_3^2) + (\tilde{M}_2^2 - \tilde{M}_3^2)) - \cos 2\theta_{12R} (3 - \cos 2\theta_{13R}) (\tilde{M}_1^2 - \tilde{M}_2^2)] \\
& \times [(m_e^2 - m_\mu^2) + (m_e^2 - m_\tau^2) + \cos 2\theta_{23L} (m_\mu^2 - m_\tau^2)] (m_\mu^2 - m_\tau^2) , \\
\Delta_7'^{(a)} &= -\frac{1}{4} d_1 d_2 (d_1^{2a} - d_2^{2a}) \cos 2\theta_{12L} \sin \theta_{13L} \sin 2\theta_{23L} \cos \theta_{13R} \cos \theta_{23R} \sin 2\theta_{12R} \\
& \times (m_\mu^2 - m_\tau^2) (\tilde{M}_1^2 - \tilde{M}_2^2) , \\
\Delta_8'^{(a)} &= \frac{1}{16} d_1 d_2 (d_1^{2a} - d_2^{2a}) \sin 2\theta_{12L} \cos \theta_{13R} \cos \theta_{23R} \sin 2\theta_{12R} (\tilde{M}_1^2 - \tilde{M}_2^2) \\
& \times [2 \cos^2 \theta_{13L} ((m_e^2 - m_\mu^2) + (m_e^2 - m_\tau^2)) - \cos 2\theta_{23L} (3 - \cos 2\theta_{13L}) (m_\mu^2 - m_\tau^2)] , \\
\Delta_9'^{(a)} &= \frac{1}{32} d_1 d_2 (d_1^{2a} - d_2^{2a}) \sin 2\theta_{12L} \sin 2\theta_{13R} \sin \theta_{23R} \\
& \times [2 \cos^2 \theta_{13L} ((m_e^2 - m_\mu^2) + (m_e^2 - m_\tau^2)) - \cos 2\theta_{23L} (3 - \cos 2\theta_{13L}) (m_\mu^2 - m_\tau^2)] \\
& \times [(\tilde{M}_1^2 - \tilde{M}_3^2) + (\tilde{M}_2^2 - \tilde{M}_3^2) + \cos 2\theta_{12R} (\tilde{M}_1^2 - \tilde{M}_2^2)] , \\
\Delta_{10}'^{(a)} &= \frac{1}{4} d_2 d_3 (d_2^{2a} - d_3^{2a}) \cos \theta_{12L} \cos \theta_{13L} \sin 2\theta_{23L} \cos 2\theta_{23R} \sin 2\theta_{12R} \sin \theta_{13R} \\
& \times (m_\mu^2 - m_\tau^2) (\tilde{M}_1^2 - \tilde{M}_2^2) , \\
\Delta_{11}'^{(a)} &= \frac{1}{4} d_1 d_3 (d_1^{2a} - d_3^{2a}) \cos \theta_{13L} \sin \theta_{12L} \sin 2\theta_{23L} \cos \theta_{13R} \sin 2\theta_{12R} \sin \theta_{23R} \\
& \times (m_\mu^2 - m_\tau^2) (\tilde{M}_1^2 - \tilde{M}_2^2) , \\
\Delta_{12}'^{(a)} &= \frac{1}{16} d_1 d_3 (d_1^{2a} - d_3^{2a}) \cos \theta_{12L} \sin 2\theta_{13L} \cos \theta_{23R} \sin 2\theta_{13R} \\
& \times [(m_e^2 - m_\mu^2) + (m_e^2 - m_\tau^2) + \cos 2\theta_{23L} (m_\mu^2 - m_\tau^2)] \\
& \times [(\tilde{M}_1^2 - \tilde{M}_3^2) + (\tilde{M}_2^2 - \tilde{M}_3^2) + \cos 2\theta_{12R} (\tilde{M}_1^2 - \tilde{M}_2^2)] .
\end{aligned}$$

References

- [1] C. Athanassopoulos *et al.* [LSND Collaboration], “Evidence for anti-muon-neutrino \rightarrow anti-electron-neutrino oscillations from the LSND experiment at LAMPF”, Phys. Rev. Lett. **77** (1996) 3082 [nucl-ex/9605003].
- [2] A. Aguilar-Arevalo *et al.* [LSND Collaboration], “Evidence for neutrino oscillations from the observation of anti-neutrino(electron) appearance in a anti-neutrino(muon) beam”, Phys. Rev. D **64** (2001) 112007 [hep-ex/0104049].
- [3] M. Tanabashi *et al.* [Particle Data Group], “Review of Particle Physics”, Phys. Rev. D **98** (2018) 030001 and 2019 update.
- [4] N. Aghanim *et al.* [Planck Collaboration], “Planck 2018 results. VI. Cosmological parameters”, arXiv:1807.06209 [astro-ph.CO].
- [5] S. Hannestad, R. S. Hansen and T. Tram, “How Self-Interactions can Reconcile Sterile Neutrinos with Cosmology” Phys. Rev. Lett. **112** (2014) no.3, 031802 [arXiv:1310.5926 [astro-ph.CO]].

- [6] B. Dasgupta and J. Kopp, “Cosmologically Safe eV-Scale Sterile Neutrinos and Improved Dark Matter Structure” *Phys. Rev. Lett.* **112** (2014) no.3, 031803 [arXiv:1310.6337 [hep-ph]].
- [7] B. Armbruster *et al.* [KARMEN Collaboration], “Upper limits for neutrino oscillations μ -on-anti-neutrino \rightarrow electron-anti-neutrino from muon decay at rest”, *Phys. Rev. D* **65** (2002) 112001 [hep-ex/0203021].
- [8] A. A. Aguilar-Arevalo *et al.* [MiniBooNE DM Collaboration], “Dark Matter Search in Nucleon, Pion, and Electron Channels from a Proton Beam Dump with MiniBooNE”, *Phys. Rev. D* **98** (2018) no.11, 112004 [arXiv:1807.06137 [hep-ex]].
- [9] M. Dentler, I. Esteban, J. Kopp and P. Machado, “Decaying Sterile Neutrinos and the Short Baseline Oscillation Anomalies”, arXiv:1911.01427 [hep-ph].
- [10] A. de Gouvêa, O. L. G. Peres, S. Prakash and G. V. Stenico, “On The Decaying-Sterile Neutrino Solution to the Electron (Anti)Neutrino Appearance Anomalies”, arXiv:1911.01447 [hep-ph].
- [11] S. Palomares-Ruiz, S. Pascoli and T. Schwetz, “Explaining LSND by a decaying sterile neutrino”, *JHEP* **0509** (2005) 048 [hep-ph/0505216].
- [12] T. A. Mueller *et al.*, “Improved Predictions of Reactor Antineutrino Spectra”, *Phys. Rev. C* **83** (2011) 054615 [arXiv:1101.2663 [hep-ex]].
- [13] G. Mention, M. Fechner, T. Lasserre, T. A. Mueller, D. Lhuillier, M. Cribier and A. Letourneau, “The Reactor Antineutrino Anomaly”, *Phys. Rev. D* **83** (2011) 073006 [arXiv:1101.2755 [hep-ex]].
- [14] P. Huber, “On the determination of anti-neutrino spectra from nuclear reactors”, *Phys. Rev. C* **84** (2011) 024617 Erratum: [*Phys. Rev. C* **85** (2012) 029901] [arXiv:1106.0687 [hep-ph]].
- [15] I. Alekseev *et al.* [DANSS Collaboration], “Search for sterile neutrinos at the DANSS experiment”, *Phys. Lett. B* **787** (2018) 56 [arXiv:1804.04046 [hep-ex]].
- [16] Y. J. Ko *et al.* [NEOS Collaboration], “Sterile Neutrino Search at the NEOS Experiment”, *Phys. Rev. Lett.* **118** (2017) no.12, 121802 [arXiv:1610.05134 [hep-ex]].
- [17] J. N. Abdurashitov *et al.*, “Measurement of the response of a Ga solar neutrino experiment to neutrinos from an Ar-37 source”, *Phys. Rev. C* **73** (2006) 045805 [nucl-ex/0512041].
- [18] M. Laveder, “Unbound neutrino roadmaps”, *Nucl. Phys. Proc. Suppl.* **168** (2007) 344.
- [19] C. Giunti and M. Laveder, “Short-Baseline Active-Sterile Neutrino Oscillations?”, *Mod. Phys. Lett. A* **22** (2007) 2499 [hep-ph/0610352].
- [20] C. Giunti and T. Lasserre, “eV-scale Sterile Neutrinos”, arXiv:1901.08330 [hep-ph].
- [21] A. Diaz, C. A. Argüelles, G. H. Collin, J. M. Conrad and M. H. Shaevitz, “Where Are We With Light Sterile Neutrinos?”, arXiv:1906.00045 [hep-ex].

- [22] P. Minkowski, “ $\mu \rightarrow e\gamma$ at a Rate of One Out of 10^9 Muon Decays?”, Phys. Lett. **67B** (1977) 421.
- [23] T. Yanagida, “Horizontal gauge symmetry and masses of neutrinos”, Conf. Proc. C **7902131** (1979) 95.
- [24] S. L. Glashow, “The Future of Elementary Particle Physics”, in Quarks and Leptons. Proceedings, Summer Institute, Cargese, France, 9 - 29 July 1979, M. Levy, J.L. Basdevant, D. Speiser, J. Weyers, R. Gastmans and M. Jacob eds., pp. 687- 713 [NATO Sci. Ser. B **61** (1980) 687].
- [25] M. Gell-Mann, P. Ramond and R. Slansky, “Complex Spinors and Unified Theories”, Conf. Proc. C **790927** (1979) 315 [arXiv:1306.4669 [hep-th]].
- [26] R. N. Mohapatra and G. Senjanovic, “Neutrino Mass and Spontaneous Parity Nonconservation”, Phys. Rev. Lett. **44** (1980) 912.
- [27] M. Fukugita and T. Yanagida, “Baryogenesis Without Grand Unification”, Phys. Lett. B **174** (1986) 45.
- [28] G. C. Branco, W. Grimus and L. Lavoura, “The Seesaw Mechanism in the Presence of a Conserved Lepton Number”, Nucl. Phys. B **312** (1989) 492.
- [29] N. R. Agostinho, G. C. Branco, P. M. F. Pereira, M. N. Rebelo and J. I. Silva-Marcos, “Can one have significant deviations from leptonic 3×3 unitarity in the framework of type I seesaw mechanism?”, Eur. Phys. J. C **78** (2018) no.11, 895 [arXiv:1711.06229 [hep-ph]].
- [30] W. Konetschny and W. Kummer, “Nonconservation of Total Lepton Number with Scalar Bosons”, Phys. Lett. **70B** (1977) 433.
- [31] J. Schechter and J. W. F. Valle, “Neutrino Masses in $SU(2) \times U(1)$ Theories”, Phys. Rev. D **22** (1980) 2227.
- [32] T. P. Cheng and L. F. Li, “Neutrino Masses, Mixings and Oscillations in $SU(2) \times U(1)$ Models of Electroweak Interactions”, Phys. Rev. D **22** (1980) 2860.
- [33] G. Lazarides, Q. Shafi and C. Wetterich, “Proton Lifetime and Fermion Masses in an $SO(10)$ Model”, Nucl. Phys. B **181** (1981) 287.
- [34] R. N. Mohapatra and G. Senjanovic, “Neutrino Masses and Mixings in Gauge Models with Spontaneous Parity Violation”, Phys. Rev. D **23** (1981) 165.
- [35] J. G. Korner, A. Pilaftsis and K. Schilcher, “Leptonic CP asymmetries in flavor changing H^0 decays”, Phys. Rev. D **47** (1993) 1080 [hep-ph/9301289].
- [36] J. A. Casas, A. Ibarra and F. Jimenez-Alburquerque, “Hints on the high-energy seesaw mechanism from the low-energy neutrino spectrum”, JHEP **0704** (2007) 064 [hep-ph/0612289].
- [37] M. Blennow and E. Fernandez-Martinez, “Parametrization of Seesaw Models and Light Sterile Neutrinos”, Phys. Lett. B **704** (2011) 223 [arXiv:1107.3992 [hep-ph]].

- [38] Z. z. Xing, “A full parametrization of the 6×6 flavor mixing matrix in the presence of three light or heavy sterile neutrinos”, Phys. Rev. D **85** (2012) 013008 [arXiv:1110.0083 [hep-ph]].
- [39] A. Donini, P. Hernandez, J. Lopez-Pavon, M. Maltoni and T. Schwetz, “The minimal 3+2 neutrino model versus oscillation anomalies”, JHEP **1207** (2012) 161 [arXiv:1205.5230 [hep-ph]].
- [40] G. C. Branco, T. Morozumi, B. M. Nobre and M. N. Rebelo, “A Bridge between CP violation at low-energies and leptogenesis” Nucl. Phys. B **617** (2001) 475 [hep-ph/0107164].
- [41] A. Broncano, M. B. Gavela and E. E. Jenkins, “The Effective Lagrangian for the seesaw model of neutrino mass and leptogenesis”, Phys. Lett. B **552** (2003) 177, Erratum: Phys. Lett. B **636** (2006) 332 [hep-ph/0210271].
- [42] G. C. Branco, R. G. Felipe and F. R. Joaquim, “Leptonic CP Violation”, Rev. Mod. Phys. **84** (2012) 515 [arXiv:1111.5332 [hep-ph]].
- [43] C. Giunti and C. W. Kim, “Fundamentals of Neutrino Physics and Astrophysics”, Oxford, UK: Univ. Pr. (2007) 710 pp.
- [44] J. A. Casas and A. Ibarra, “Oscillating neutrinos and $\mu \rightarrow e, \gamma$ ”, Nucl. Phys. B **618** (2001) 171 [hep-ph/0103065].
- [45] J. Gluza, “On teraelectronvolt Majorana neutrinos”, Acta Phys. Polon. B **33** (2002) 1735 [hep-ph/0201002].
- [46] S. Antusch, C. Biggio, E. Fernandez-Martinez, M. B. Gavela and J. Lopez-Pavon, “Unitarity of the Leptonic Mixing Matrix”, JHEP **0610** (2006) 084 [hep-ph/0607020].
- [47] E. Fernandez-Martinez, M. B. Gavela, J. Lopez-Pavon and O. Yasuda, “CP-violation from non-unitary leptonic mixing”, Phys. Lett. B **649** (2007) 427 [hep-ph/0703098].
- [48] S. Antusch and O. Fischer, “Non-unitarity of the leptonic mixing matrix: Present bounds and future sensitivities”, JHEP **1410** (2014) 094 [arXiv:1407.6607 [hep-ph]].
- [49] E. Fernandez-Martinez, J. Hernandez-Garcia and J. Lopez-Pavon, “Global constraints on heavy neutrino mixing”, JHEP **1608** (2016) 033 [arXiv:1605.08774 [hep-ph]].
- [50] M. Blennow, P. Coloma, E. Fernandez-Martinez, J. Hernandez-Garcia and J. Lopez-Pavon, “Non-Unitarity, sterile neutrinos, and Non-Standard neutrino Interactions”, JHEP **1704** (2017) 153 [arXiv:1609.08637 [hep-ph]].
- [51] Y. Declais *et al.*, “Search for neutrino oscillations at 15-meters, 40-meters, and 95-meters from a nuclear power reactor at Bugey”, Nucl. Phys. B **434** (1995) 503.
- [52] P. Adamson *et al.* [MINOS Collaboration], “Search for Sterile Neutrinos Mixing with Muon Neutrinos in MINOS”, Phys. Rev. Lett. **117** (2016) no.15, 151803 [arXiv:1607.01176 [hep-ex]].

- [53] P. Astier *et al.* [NOMAD Collaboration], “Final NOMAD results on muon-neutrino \rightarrow tau-neutrino and electron-neutrino \rightarrow tau-neutrino oscillations including a new search for tau-neutrino appearance using hadronic tau decays”, Nucl. Phys. B **611** (2001) 3 [hep-ex/0106102].
- [54] P. Astier *et al.* [NOMAD Collaboration], “Search for $\nu_\mu \rightarrow \nu_e$ oscillations in the NOMAD experiment”, Phys. Lett. B **570** (2003) 19 [hep-ex/0306037].
- [55] K. Abe *et al.* [Super-Kamiokande Collaboration], “Limits on sterile neutrino mixing using atmospheric neutrinos in Super-Kamiokande”, Phys. Rev. D **91** (2015) 052019 [arXiv:1410.2008 [hep-ex]].
- [56] M. Drewes *et al.*, “A White Paper on keV Sterile Neutrino Dark Matter”, JCAP **1701** (2017) 025 [arXiv:1602.04816 [hep-ph]].
- [57] S. Antusch and O. Fischer, “Testing sterile neutrino extensions of the Standard Model at future lepton colliders”, JHEP **1505** (2015) 053 [arXiv:1502.05915 [hep-ph]].
- [58] F. F. Deppisch, P. S. Bhupal Dev and A. Pilaftsis, “Neutrinos and Collider Physics,” New J. Phys. **17** (2015) no.7, 075019 [arXiv:1502.06541 [hep-ph]].
- [59] A. Das and N. Okada, “Improved bounds on the heavy neutrino productions at the LHC”, Phys. Rev. D **93** (2016) no.3, 033003 [arXiv:1510.04790 [hep-ph]].
- [60] A. Das and N. Okada, “Bounds on heavy Majorana neutrinos in type-I seesaw and implications for collider searches”, Phys. Lett. B **774** (2017) 32 [arXiv:1702.04668 [hep-ph]].
- [61] A. Das, P. S. B. Dev and C. S. Kim, “Constraining Sterile Neutrinos from Precision Higgs Data”, Phys. Rev. D **95** (2017) no.11, 115013 [arXiv:1704.00880 [hep-ph]].
- [62] A. M. Sirunyan *et al.* [CMS Collaboration], “Search for heavy neutral leptons in events with three charged leptons in proton-proton collisions at $\sqrt{s} = 13$ TeV”, Phys. Rev. Lett. **120** (2018) no.22, 221801 [arXiv:1802.02965 [hep-ex]].
- [63] A. M. Sirunyan *et al.* [CMS Collaboration], “Search for heavy Majorana neutrinos in same-sign dilepton channels in proton-proton collisions at $\sqrt{s} = 13$ TeV”, JHEP **1901** (2019) 122 [arXiv:1806.10905 [hep-ex]].
- [64] A. M. Baldini *et al.* [MEG Collaboration], “Search for the lepton flavour violating decay $\mu^+ \rightarrow e^+ \gamma$ with the full dataset of the MEG experiment”, Eur. Phys. J. C **76** (2016) no.8, 434 [arXiv:1605.05081 [hep-ex]].
- [65] N. Aghanim *et al.* [Planck Collaboration], “Planck intermediate results. XLVI. Reduction of large-scale systematic effects in HFI polarization maps and estimation of the reionization optical depth”, Astron. Astrophys. **596** (2016) A107 [arXiv:1605.02985 [astro-ph.CO]].
- [66] G. Cozzella and C. Giunti, “Mixed states for mixing neutrinos”, Phys. Rev. D **98** (2018) no.9, 096010 [arXiv:1804.00184 [hep-ph]].
- [67] P. Langacker and D. London, “Mixing Between Ordinary and Exotic Fermions”, Phys. Rev. D **38** (1988) 886.

- [68] W. Grimus and L. Lavoura, “One-loop corrections to the seesaw mechanism in the multi-Higgs-doublet standard model”, *Phys. Lett. B* **546** (2002) 86 [hep-ph/0207229].
- [69] D. Aristizabal Sierra and C. E. Yaguna, “On the importance of the 1-loop finite corrections to seesaw neutrino masses”, *JHEP* **1108** (2011) 013. [arXiv:1106.3587 [hep-ph]].
- [70] W. Grimus and M. Löschner, “Renormalization of the multi-Higgs-doublet Standard Model and one-loop lepton mass corrections”, *JHEP* **1811** (2018) 087 [arXiv:1807.00725 [hep-ph]].
- [71] M. Shaposhnikov, “A Possible symmetry of the nuMSM”, *Nucl. Phys. B* **763** (2007) 49 [hep-ph/0605047].
- [72] J. Kersten and A. Y. Smirnov, “Right-Handed Neutrinos at CERN LHC and the Mechanism of Neutrino Mass Generation”, *Phys. Rev. D* **76** (2007) 073005 [arXiv:0705.3221 [hep-ph]].
- [73] A. Ibarra, E. Molinaro and S. T. Petcov, “TeV Scale See-Saw Mechanisms of Neutrino Mass Generation, the Majorana Nature of the Heavy Singlet Neutrinos and $(\beta\beta)_{0\nu}$ -Decay”, *JHEP* **1009** (2010) 108 [arXiv:1007.2378 [hep-ph]].
- [74] L. Lavoura and W. Grimus, “Seesaw model with softly broken $L(e) - L(\mu) - L(\tau)$ ”, *JHEP* **0009** (2000) 007 [hep-ph/0008020].
- [75] W. Grimus and L. Lavoura, “Softly broken lepton numbers and maximal neutrino mixing”, *JHEP* **0107** (2001) 045 [hep-ph/0105212].
- [76] L. Wolfenstein, “Different Varieties of Massive Dirac Neutrinos”, *Nucl. Phys. B* **186** (1981) 147.
- [77] C. N. Leung and S. T. Petcov, “A Comment on the Coexistence of Dirac and Majorana Massive Neutrinos”, *Phys. Lett.* **125B** (1983) 461.
- [78] S. T. Petcov, “On Pseudodirac Neutrinos, Neutrino Oscillations and Neutrinoless Double beta Decay”, *Phys. Lett.* **110B** (1982) 245.
- [79] A. Ibarra, E. Molinaro and S. T. Petcov, “Low Energy Signatures of the TeV Scale See-Saw Mechanism,”, *Phys. Rev. D* **84** (2011) 013005 [arXiv:1103.6217 [hep-ph]].
- [80] D. N. Dinh, A. Ibarra, E. Molinaro and S. T. Petcov, “The $\mu - e$ Conversion in Nuclei, $\mu \rightarrow e\gamma, \mu \rightarrow 3e$ Decays and TeV Scale See-Saw Scenarios of Neutrino Mass Generation”, *JHEP* **1208** (2012) 125, Erratum: *JHEP* **1309** (2013) 023 [arXiv:1205.4671 [hep-ph]].
- [81] C. G. Cely, A. Ibarra, E. Molinaro and S. T. Petcov, “Higgs Decays in the Low Scale Type I See-Saw Model”, *Phys. Lett. B* **718** (2013) 957 [arXiv:1208.3654 [hep-ph]].
- [82] J. T. Penedo, S. T. Petcov and T. Yanagida, “Low-Scale Seesaw and the CP Violation in Neutrino Oscillations”, *Nucl. Phys. B* **929** (2018) 377 [arXiv:1712.09922 [hep-ph]].
- [83] P. F. De Salas, S. Gariazzo, O. Mena, C. A. Ternes and M. Třářtola, “Neutrino Mass Ordering from Oscillations and Beyond: 2018 Status and Future Prospects”, *Front. Astron. Space Sci.* **5** (2018) 36 [arXiv:1806.11051 [hep-ph]].

- [84] I. Esteban, M. C. Gonzalez-Garcia, A. Hernandez-Cabezudo, M. Maltoni and T. Schwetz, “Global analysis of three-flavour neutrino oscillations: synergies and tensions in the determination of θ_{23} , δ_{CP} , and the mass ordering”, JHEP **1901** (2019) 106 [arXiv:1811.05487 [hep-ph]].
- [85] S. Gariazzo, C. Giunti, M. Laveder, Y. F. Li and E. M. Zavanin, “Light sterile neutrinos”, J. Phys. G **43** (2016) 033001 [arXiv:1507.08204 [hep-ph]].
- [86] A. Boyarsky, M. Drewes, T. Lasserre, S. Mertens and O. Ruchayskiy, “Sterile Neutrino Dark Matter”, Prog. Part. Nucl. Phys. **104** (2019) 1 [arXiv:1807.07938 [hep-ph]].
- [87] DUNE Collaboration, “Long-Baseline Neutrino Facility (LBNF) and Deep Underground Neutrino Experiment (DUNE): Conceptual Design Report, Vols. 1-4”, arXiv:1601.05471, arXiv:1512.06148, arXiv:1601.05823, arXiv:1601.02984 [physics.ins-det].
- [88] M. Antonello *et al.* [MicroBooNE, LAr1-ND and ICARUS-WA104 Collaborations], “A Proposal for a Three Detector Short-Baseline Neutrino Oscillation Program in the Fermilab Booster Neutrino Beam”, arXiv:1503.01520 [physics.ins-det].
- [89] S. Vagnozzi, E. Giusarma, O. Mena, K. Freese, M. Gerbino, S. Ho and M. Lattanzi, “Unveiling ν secrets with cosmological data: neutrino masses and mass hierarchy”, Phys. Rev. D **96** (2017) no.12, 123503 [arXiv:1701.08172 [astro-ph.CO]].
- [90] A. S. Riis and S. Hannestad, “Detecting sterile neutrinos with KATRIN like experiments”, JCAP **1102** (2011) 011 [arXiv:1008.1495 [astro-ph.CO]].
- [91] S. Mertens *et al.*, “Sensitivity of Next-Generation Tritium Beta-Decay Experiments for keV-Scale Sterile Neutrinos”, JCAP **1502** (2015) 020 [arXiv:1409.0920 [physics.ins-det]].
- [92] P. W. Cattaneo [MEG II Collaboration], “The MEGII detector”, JINST **12** (2017) C06022 [arXiv:1705.10224 [physics.ins-det]].
- [93] J. D. Vergados, H. Ejiri and F. Šimkovic, “Neutrinoless double beta decay and neutrino mass”, Int. J. Mod. Phys. E **25** (2016) no.11, 1630007 [arXiv:1612.02924 [hep-ph]].
- [94] S. Antusch, E. Cazzato and O. Fischer, “Sterile neutrino searches at future e^-e^+ , pp , and e^-p colliders”, Int. J. Mod. Phys. A **32** (2017) no.14, 1750078 [arXiv:1612.02728 [hep-ph]].
- [95] S. Antusch, E. Cazzato and O. Fischer, “Displaced vertex searches for sterile neutrinos at future lepton colliders”, JHEP **1612** (2016) 007 [arXiv:1604.02420 [hep-ph]].
- [96] S. Antusch, E. Cazzato and O. Fischer, “Resolvable heavy neutrino–antineutrino oscillations at colliders”, Mod. Phys. Lett. A **34** (2019) no.07n08, 1950061 [arXiv:1709.03797 [hep-ph]].
- [97] A. Pilaftsis and T. E. J. Underwood, “Resonant leptogenesis”, Nucl. Phys. B **692** (2004) 303 [hep-ph/0309342].
- [98] A. Abada, G. Arcadi, V. Domcke and M. Lucente, “Neutrino masses, leptogenesis and dark matter from small lepton number violation?”, JCAP **1712** (2017) 024 [arXiv:1709.00415 [hep-ph]].

- [99] R. Gandhi, B. Kayser, M. Masud and S. Prakash, “The impact of sterile neutrinos on CP measurements at long baselines”, JHEP **1511** (2015) 039 [arXiv:1508.06275 [hep-ph]].
- [100] Y. Reyimuaji and C. Liu, “Prospects of light sterile neutrino searches in long-baseline experiments”, arXiv:1911.12524 [hep-ph].
- [101] J. Bernabeu, G. C. Branco and M. Gronau, “CP Restrictions on Quark Mass Matrices”, Phys. Lett. **169B** (1986) 243.
- [102] G. C. Branco, L. Lavoura and J. P. Silva, “CP Violation”, Int. Ser. Monogr. Phys. **103** (1999) 1.
- [103] G. C. Branco, L. Lavoura and M. N. Rebelo, “Majorana Neutrinos and CP Violation in the Leptonic Sector”, Phys. Lett. B **180** (1986) 264.
- [104] A. Pilaftsis, “CP violation and baryogenesis due to heavy Majorana neutrinos”, Phys. Rev. D **56** (1997) 5431 [hep-ph/9707235].
- [105] G. C. Branco, M. N. Rebelo and J. I. Silva-Marcos, “Degenerate and quasidegenerate Majorana neutrinos”, Phys. Rev. Lett. **82** (1999) 683 [hep-ph/9810328].
- [106] S. Davidson and R. Kitano, “Leptogenesis and a Jarlskog invariant”, JHEP **0403** (2004) 020 [hep-ph/0312007].
- [107] G. C. Branco, M. N. Rebelo and J. I. Silva-Marcos, “Leptogenesis, Yukawa textures and weak basis invariants”, Phys. Lett. B **633** (2006) 345 [hep-ph/0510412].
- [108] H. K. Dreiner, J. S. Kim, O. Lebedev and M. Thormeier, “Supersymmetric Jarlskog invariants: The Neutrino sector”, Phys. Rev. D **76** (2007) 015006 [hep-ph/0703074 [HEP-PH]].
- [109] Y. Wang and Z. z. Xing, “Commutators of lepton mass matrices associated with the seesaw and leptogenesis mechanisms”, Phys. Rev. D **89** (2014) no.9, 097301 [arXiv:1404.0109 [hep-ph]].